LETTER

doi:10.1038/nature12331

T_{reg} induction by a rationally selected mixture of Clostridia strains from the human microbiota

Koji Atarashi[1,2,3]*, Takeshi Tanoue[1,2]*, Kenshiro Oshima[4,5]*, Wataru Suda[5], Yuji Nagano[1,2], Hiroyoshi Nishikawa[6], Shinji Fukuda[1,7], Takuro Saito[6], Seiko Narushima[1], Koji Hase[1,3], Sangwan Kim[5], Joëlle V. Fritz[8], Paul Wilmes[8], Satoshi Ueha[9], Kouji Matsushima[9], Hiroshi Ohno[1], Bernat Olle[10], Shimon Sakaguchi[6], Tadatsugu Taniguchi[2], Hidetoshi Morita[4,11], Masahira Hattori[5] & Kenya Honda[1,2,4]

Manipulation of the gut microbiota holds great promise for the treatment of inflammatory and allergic diseases[1,2]. Although numerous probiotic microorganisms have been identified[3], there remains a compelling need to discover organisms that elicit more robust therapeutic responses, are compatible with the host, and can affect a specific arm of the host immune system in a well-controlled, physiological manner. Here we use a rational approach to isolate $CD4^+FOXP3^+$ regulatory T (T_{reg})-cell-inducing bacterial strains from the human indigenous microbiota. Starting with a healthy human faecal sample, a sequence of selection steps was applied to obtain mice colonized with human microbiota enriched in T_{reg}-cell-inducing species. From these mice, we isolated and selected 17 strains of bacteria on the basis of their high potency in enhancing T_{reg} cell abundance and inducing important anti-inflammatory molecules—including interleukin-10 (IL-10) and inducible T-cell co-stimulator (ICOS)—in T_{reg} cells upon inoculation into germ-free mice. Genome sequencing revealed that the 17 strains fall within clusters IV, XIVa and XVIII of Clostridia, which lack prominent toxins and virulence factors. The 17 strains act as a community to provide bacterial antigens and a TGF-β-rich environment to help expansion and differentiation of T_{reg} cells. Oral administration of the combination of 17 strains to adult mice attenuated disease in models of colitis and allergic diarrhoea. Use of the isolated strains may allow for tailored therapeutic manipulation of human immune disorders.

$CD4^+FOXP3^+$ T_{reg} cells are present most abundantly in the intestinal mucosa at steady state, and contribute to intestinal and systemic immune homeostasis[4–7]. In germ-free mice, the frequency of colonic T_{reg} cells and levels of IL-10 expression by T_{reg} cells are markedly reduced[4–7]. We have shown previously that a combination of Clostridia strains isolated from conventionally reared mice potently affect the number and function of $CD4^+FOXP3^+$ T_{reg} cells in mouse colonic lamina propria[4]. In an attempt to enable clinical translation of our previous findings, we aimed to identify T_{reg}-cell-inducing bacterial strains derived from the human microbiota (see Supplementary Fig. 1 for a summary of the procedure).

We obtained a human stool sample from a healthy Japanese volunteer. Because we previously reported that the chloroform-resistant fraction of mouse gut microbiota was enriched in T_{reg}-cell-inducing species[4], the stool sample was either untreated or treated with chloroform and orally inoculated into IQI/Jic germ-free mice. Each group of ex-germ-free (exGF) mice was separately housed for 3–4 weeks in vinyl isolators to avoid further microbial contamination. Although a recent study showed that the human microbiota had no impact on the immune responses in the mouse small intestine[8], we observed a significant increase in the percentage of $FOXP3^+$ T_{reg} cells among $CD4^+$ T cells in the colons of exGF mice inoculated with untreated human faeces compared with germ-free mice (Fig. 1a and Supplementary Fig. 2). Notably, a more pronounced increase was observed in the colons of exGF mice inoculated with chloroform-treated human faeces (Fig. 1a). These findings suggest that the human intestinal microbiota contains T_{reg}-cell-inducing bacteria, and that they are enriched in the chloroform-resistant fraction. We also examined the effects of human faeces inoculation on colonic IL-17- and IFN-γ-expressing $CD4^+$ cells (T_H17 and T_H1 cells). In exGF mice inoculated with untreated or chloroform-treated human faeces, the frequency of T_H1 cells was unchanged compared with germ-free mice (Fig. 1b). By contrast, there

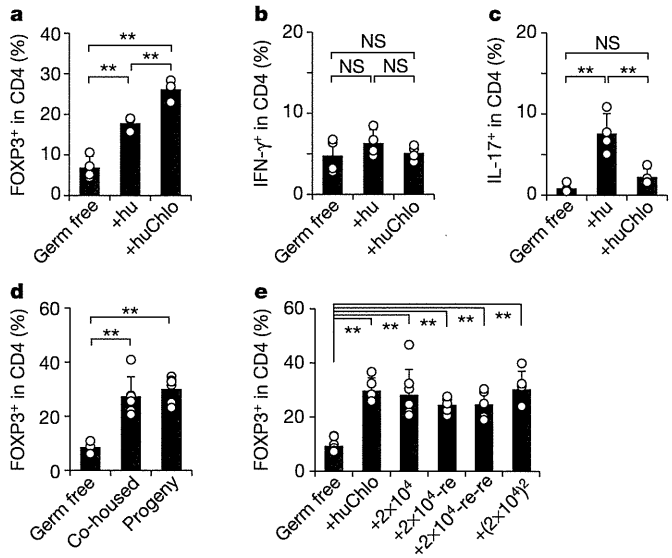

Figure 1 | T_{reg} cell accumulation in germ-free mice induced by inoculation with human microbiota. a–e, The percentages of $FOXP3^+$, $IL\text{-}17^+$ and $IFN\text{-}\gamma^+$ cells within the $CD4^+$ cell population in the colon lamina propria of the indicated mice are shown (see also Supplementary Fig. 2). Circles represent individual animals. The height of the black bars indicates the mean. All experiments were performed more than twice with similar results. Error bars indicate s.d. $^{**}P < 0.01$; NS, not significant. +hu, exGF mice inoculated with untreated human faeces; +huChlo, exGF mice inoculated with chloroform-treated human faeces. (See the main text for further definitions of *x*-axis labels.)

[1]RIKEN Center for Integrative Medical Sciences (IMS-RCAI), 1-7-22 Suehiro-cho, Tsurumi-ku, Yokohama, Kanagawa 230-0045, Japan. [2]Department of Immunology, Graduate School of Medicine, The University of Tokyo, 7-3-1 Hongo, Bunkyo-ku, Tokyo 113-0033, Japan. [3]PRESTO, Japan Science and Technology Agency, 4-1-8 Honcho Kawaguchi, Saitama 332-0012, Japan. [4]CREST, Japan Science and Technology Agency, 4-1-8 Honcho Kawaguchi, Saitama 332-0012, Japan. [5]Graduate School of Frontier Sciences, The University of Tokyo, 5-1-5 Kashiwanoha, Kashiwa, Chiba 277-8561, Japan. [6]Experimental Immunology, Immunology Frontier Research Center, Osaka University, 3-1 Yamadaoka, Suita, Osaka 565-0871, Japan. [7]Institute for Advanced Biosciences, Keio University, 246-2 Mizukami, Tsuruoka, Yamagata 997-0052, Japan. [8]Luxembourg Centre for Systems Biomedicine, University of Luxembourg, Avenue des Hauts-Fourneaux, 7, Esch-sur-Alzette, L-4362, Luxembourg. [9]Department of Molecular Preventive Medicine, Graduate School of Medicine, The University of Tokyo, 7-3-1 Hongo, Bunkyo-ku, Tokyo 113-0033, Japan. [10]PureTech Ventures, 500 Boylston Street, Suite 1600, Boston, Massachusetts 02116, USA. [11]School of Veterinary Medicine, Azabu University, 1-17-71 Fuchinobe, Sagamihara, Kanagawa 252-5201, Japan.
*These authors contributed equally to this work.

was a significant accumulation of T_H17 cells in the colons of exGF mice inoculated with untreated human faeces (Fig. 1c and Supplementary Fig. 2). Notably, the capacity of human faeces to induce T_H17 cells was greatly diminished after treatment with chloroform (Fig. 1c). These results indicate that the chloroform-sensitive bacterial fraction in the human stool tested contained T_H17-cell-inducing bacteria, whereas the chloroform-resistant bacteria preferentially promoted T_{reg} cell accumulation in the colon.

To investigate whether T_{reg} cell induction by the chloroform-resistant fraction of human intestinal bacteria is transmissible, adult germ-free mice were co-housed with exGF mice inoculated with chloroform-treated human faeces for 4 weeks. Co-housed mice showed a significant increase in the frequency of colonic T_{reg} cells (Fig. 1d). In addition, the progeny of exGF mice inoculated with chloroform-treated human faeces also showed increased numbers of T_{reg} cells (Fig. 1d). Therefore, T_{reg} cell induction by human intestinal bacteria is horizontally and vertically transmissible. Oral inoculation of germ-free mice with 2×10^4-fold diluted caecal samples from exGF mice inoculated with chloroform-treated human faeces fully induced the accumulation of T_{reg} cells in the colon lamina propria, suggesting that abundant rather than minor members of the intestinal microbiota in exGF mice inoculated with chloroform-treated human faeces drive the observed induction of T_{reg} cells (Fig. 1e). The T_{reg}-cell-inducing microbiota in mice inoculated with the 2×10^4-fold diluted sample ($+2 \times 10^4$ mice) was a stable community, because serial oral inoculation of caecal contents from these mice equally induced the accumulation of T_{reg} cells in secondary ($+2\times10^4$-re mice) and tertiary recipients ($+2\times10^4$-re-re mice) (Fig. 1e). To minimize nonessential components of the microbiota for T_{reg} cell induction, the caecal contents of $+2 \times 10^4$ mice were again diluted 2×10^4-fold and orally inoculated into another set of germ-free mice ($+(2 \times 10^4)^2$ mice). The $+(2 \times 10^4)^2$ mice had a marked accumulation of T_{reg} cells in the colon (Fig. 1e). These results suggested that we succeeded in obtaining mice colonized with a relatively restricted and stable community of bacterial species enriched for T_{reg} cell inducers.

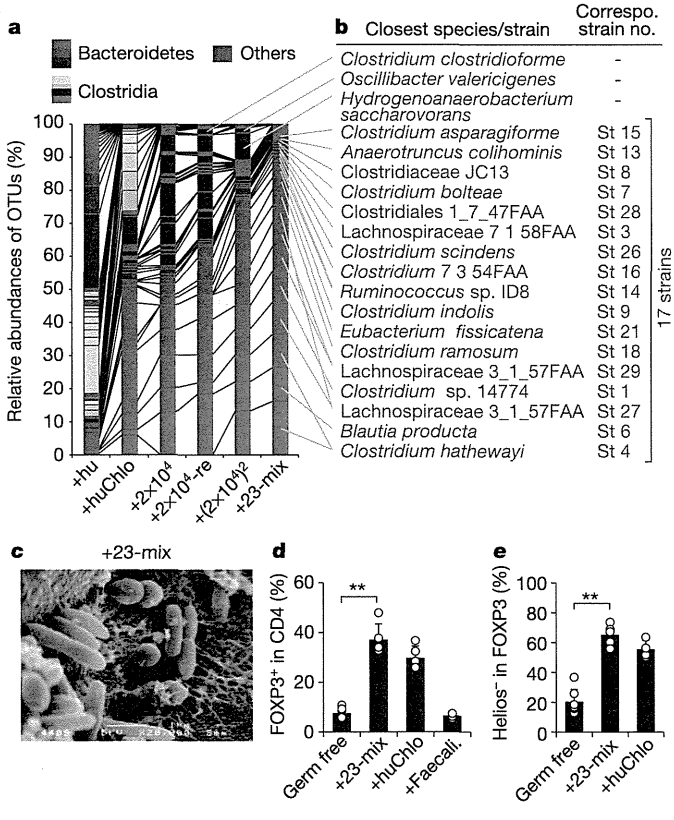

Figure 2 | Assessment of microbiota composition and isolation of T_{reg}-cell-inducing strains. a, b, Pyrosequencing of 16S rRNA genes was performed on caecal contents from the indicated mice. Relative abundance of OTUs (%) in the caecal bacterial community in each mouse (**a**), and the closest species/strain in the database and the corresponding isolated strain number for the indicated OTU (**b**) are shown. **c**, SEM showing the proximal colon of +23-mix mice. Original magnification, ~×20,000. **d, e**, The percentages of $FOXP3^+$ cells within the $CD4^+$ cell population (**d**) and $Helios^-$ cells in $CD4^+FOXP3^+$ cells (**e**) in the colon of the indicated mice. Circles represent individual animals. All experiments were performed more than twice with similar results. Error bars indicate s.d. $^{**}P < 0.01$.

The composition of the gut microbiota in mice treated with human samples was analysed by 16S ribosomal RNA (rRNA) gene amplicon sequencing using a 454 sequencer. Quality filter-passed sequences (3,000 reads for each sample) were classified into operational taxonomic units (OTUs) based on sequence similarity (>96% identity). The numbers of detected reads and closest known species for each OTU are shown in Supplementary Table 1, and the relative abundance of OTUs in each caecal sample is shown in Fig. 2a. As expected, the OTU profiles of mice treated with human faeces were quite different from those of conventional specific pathogen-free (SPF) mice (Supplementary Fig. 3). In mice inoculated with untreated human faeces, OTUs belonging to Bacteroidetes accounted for about 50% of the caecal microbial community (Fig. 2a). By contrast, most OTUs in exGF mice inoculated with chloroform-treated human faeces were related to Clostridia species. Most bacteria in $+2 \times 10^4$, $+2 \times 10^4$-re and $+(2 \times 10^4)^2$ mice had 16S rRNA gene sequence similarities with about 20 species of Clostridia, listed in Fig. 2b.

To isolate bacterial strains with T_{reg}-cell-inducing capabilities, we cultured caecal contents from $+2 \times 10^4$, $+2 \times 10^4$-re and $+(2 \times 10^4)^2$ mice *in vitro* and picked 442 colonies. BLAST searches of 16S rRNA gene sequences of the isolated colonies revealed that 31 strains in total were present, all of which were Clostridia (Supplementary Fig. 4). Of the 31 strains, we selected 23 that had less than 99% 16S rRNA gene sequence identity to any of the other 30 strains (Supplementary Fig. 4). We then individually cultured the 23 strains, mixed them in equal amounts, and orally inoculated the mixture into germ-free IQI mice (+23-mix mice). Numerous rod- and round-shaped bacteria were observed by scanning electron microscopy (SEM) on the epithelial cell surface in +23-mix mice (Fig. 2c), and the size and appearance of the caeca were quite different from those in germ-free mice, indicating successful colonization (Supplementary Fig. 5a). Pyrosequencing of 16S rRNA genes revealed that the caecal microbiota composition in +23-mix mice was quite similar to that in $+(2 \times 10^4)^2$ mice (Fig. 2a). In +23-mix mice, we observed efficient induction of T_{reg} cells in the colonic lamina propria (Fig. 2d). The magnitude was comparable to that observed in exGF mice inoculated with chloroform-treated human faeces and much higher than that in mice colonized with *Faecalibacterium prausnitzii*, a human Clostridia strain well known for enhancing regulatory cell functions[9] (Fig. 2d). Most T_{reg} cells in +23-mix mice expressed low levels of Helios (also known as IKZF2), indicating antigen-experienced cells (Fig. 2e, Supplementary Fig. 5b and ref. 10).

Only 17 strains listed in Fig. 2b and Supplementary Fig. 4 were detected in +23-mix mice by 16S rRNA gene sequencing, indicating that these 17 strains may be sufficient to induce T_{reg} cells. Indeed, we found that the mixture of 17 strains (17-mix) induced $FOXP3^+$ T_{reg} cells to a similar extent as the 23-mix (Fig. 3a). The increase in T_{reg} cells induced by the 17-mix was reproducibly observed in exGF mice of different genetic backgrounds (IQI, BALB/c and C57BL/6) (Fig. 3a). Moreover, the mix was effective in other rodents: the frequency of colonic T_{reg} cells in exGF rats inoculated with 17-mix was significantly higher than that in germ-free rats and comparable to that in SPF rats (Fig. 3a). The colonization with 17-mix induced a significant increase in the frequency of IL-10^+ and/or $ICOS^+$ cells within the T_{reg} cell population, as revealed by analysis of exGF IL-10 reporter mice (*Il10*^{Venus} mice, ref. 4) colonized with the 17-mix (Fig. 3b). Furthermore, IL-10^+ T_{reg} cells in

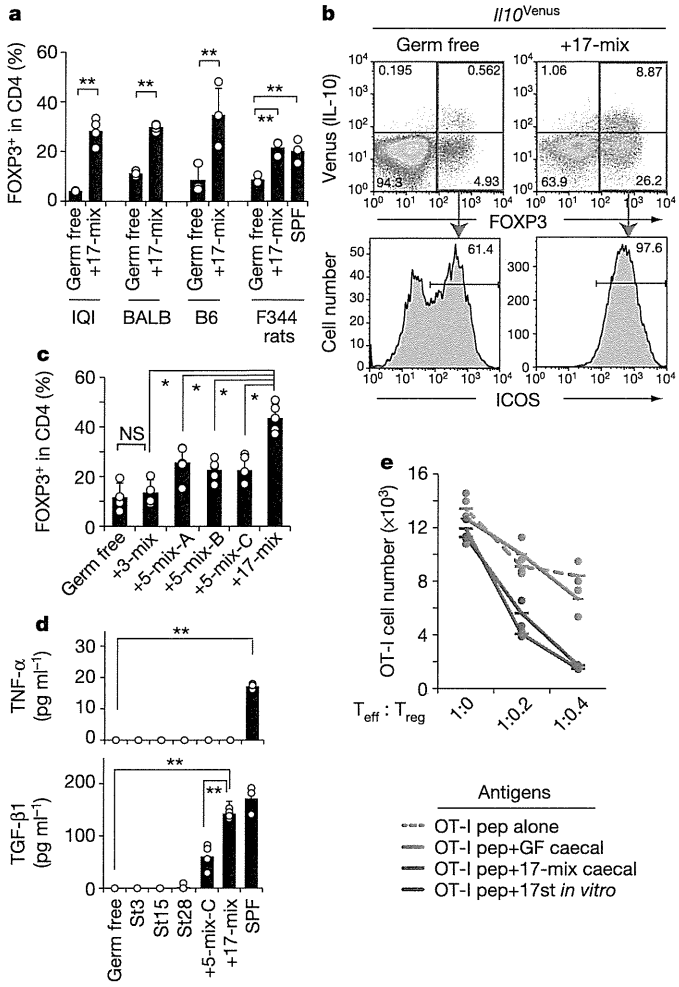

Figure 3 | Characterization of 17 T_{reg}-cell-inducing strains. **a**, The percentages of $FOXP3^+$ cells within the $CD4^+$ cell population in the colon lamina propria of the indicated mice and rats. **b**, The expression of Venus (IL-10) and FOXP3 by the gated colonic lamina propria $CD4^+$ cells, and ICOS expression by $CD4^+FOXP3^+$ cells in exGF *Il10*^{Venus} mice colonized with or without 17-mix. **c**, Percentages of $FOXP3^+$ cells within the $CD4^+$ cell population in IQI exGF mice colonized with the indicated mix. **d**, The production of TNF-α and TGF-β1 in HCT8 cells stimulated with caecal extracts from the indicated mice. **e**, $CD8^+$ T cells from OT-I mice (T_{eff}) and the indicated ratio of colon lamina propria $CD4^+CD25^+$ cells from +17-mix mice (T_{reg}) were incubated with $CD11c^+$ cells pulsed with OT-I peptide alone or in combination with autoclaved caecal contents from +17-mix mice (+17-mix caecal), germ-free mice (+GF caecal), or autoclaved 17 strains cultured *in vitro* (+17 st *in vitro*). Depicted data represent average of duplicates (see also Supplementary Fig. 9c). Circles in **a**, **c**–**e** represent samples from individual animals. All experiments were performed more than twice with similar results. Error bars indicate s.d. $^{**}P < 0.01$; $^{*}P < 0.05$; NS, not significant.

+17-mix mice expressed high levels of CTLA4 (Supplementary Fig. 5c). Because IL-10 and CTLA4 are essential for the immunosuppressive activity of T_{reg} cells[11,12], and ICOS is required for the T_{reg}-cell-mediated suppression of T_H2 responses[13], these results suggest that the mixture of 17 strains affects both the number and function of T_{reg} cells in the colon. Next, we monocolonized germ-free mice with one of each of the 17 individual strains to determine their individual T_{reg} cell induction capability. The monocolonized exGF mice exhibited low to intermediate levels of T_{reg} cell induction with inter-individual variability (Supplementary Fig. 6a). As expected, none of the strains induced T_H17 cells in the monocolonized mice (Supplementary Fig. 6b). We also examined T_{reg} cell induction by subsets of the 17-mix (randomly selected combinations of 3–5 strains: 3-mix, 5-mix-A, 5-mix-B, and 5-mix-C, see Supplementary Fig. 4). Although all tested combinations of 5-mix induced increases in the frequency of T_{reg} cells, the magnitude was substantially lower than that observed in +17-mix mice (Fig. 3c). Therefore, it is likely that the 17 strains act synergistically to amplify the induction of T_{reg} cells in a microbial-community-dependent fashion.

To investigate the mechanism for the T_{reg} cell induction by the community of 17 strains, we incubated various human and mouse intestinal epithelial cell lines and primary cells with aqueous extracts from caecal contents from the +17-mix mice, and assessed the production of the active form of TGF-β1, a key cytokine for the differentiation and expansion of T_{reg} cells. The caecal extracts from +17-mix mice routinely elicited TGF-β1, but not IL-6 and TNF-α, production, and the magnitude was significantly higher than that elicited by caecal extracts from single-strain or 5-mix-colonized mice (Fig. 3d and Supplementary Fig. 7). The induction of TGF-β1 was not inhibited by pre-treatment of the caecal extracts with a protease or nuclease (Supplementary Fig. 7c). Short-chain fatty acids (SCFAs) are protease- and nuclease-insensitive and have been associated with regulation of host immune homeostasis[14]. Quantitative analysis of SCFAs in caecal contents from +17-mix mice showed a significantly higher concentration of acetate, propionate, butyrate and isobutyrate than that in single-strain or 5-mix-colonized mice (Supplementary Fig. 8a). Furthermore, a mixture of sodium salts of these SCFAs elicited TGF-β1 production in epithelial cells to a level similar to that seen when the cells were stimulated with caecal extracts from +17-mix mice (Supplementary Fig. 8b). Therefore, the community of 17 strains cooperatively produces SCFAs that can elicit a TGF-β response, and this activity may contribute to the differentiation and expansion of T_{reg} cells. We also investigated whether the 17 strains provide bacterial antigens to T cells. To do this, we addressed the antigen specificity of T_{reg} cells accumulated in +17-mix mice using a cognate antigen-driven suppression assay. $CD4^+CD25^+$ lamina propria T cells from +17-mix mice substantially inhibited the OT-I ovalbumin (OVA) peptide-driven proliferation of OT-I CD8 T cells, and this suppression was markedly enhanced in the presence of autoclaved caecal content from +17-mix mice or autoclaved 17 strains cultured *in vitro*, but not in the presence of OT-II OVA peptide or caecal content from germ-free mice (Fig. 3e and Supplementary Fig. 9). These results are consistent with previous reports[15,16] and suggest that some fraction of colonic lamina propria T_{reg} cells in +17-mix mice is specific to the 17 strains of Clostridia. Next, we assessed the kinetics of T_{reg} cell accumulation and their expression of Ki67, a cell-cycle-associated nuclear protein, and gut-homing-associated molecules CD103 and β7 integrin. We observed a marked increase in the proportion of Ki67, CD103 and β7 expressing cells by 1 week after inoculation with the 17-mix (Supplementary Figs 10 and 11). Collectively, these observations indicate that the 17 strains provide SCFAs, bacterial antigens and probably other factors, which together contribute to differentiation, expansion and colonic homing of T_{reg} cells.

To define the identity of the 17 bacterial strains fully, we sequenced their genomes (Supplementary Fig. 12). Phylogenetic comparison of the 17 strains using ribosomal multi locus sequencing typing (rMLST) revealed that the 17 strains belong to bacterial species falling within clusters XIVa, IV and XVIII of Clostridia as defined previously[17] (in a recent taxonomy, members of cluster XVIII Clostridia were reclassified in the class Erysipelotrichi) (Supplementary Fig. 13). The genome sequencing also revealed that the 17 strains all lack strong virulence-related genes such as collagenase and phospholipase C, often identified in pathogenic Clostridia species (Supplementary Table 2). We then examined the relative abundance of the 17 strains in healthy and ulcerative colitis human subjects using draft genome sequences of the 17 strains and publicly available human microbiome genomes generated through the MetaHIT project[18]. Ulcerative colitis subjects showed a tendency towards a reduction of the 17 strains, and 5 out of the 17 strains were significantly reduced in ulcerative colitis patients (Supplementary Fig. 14).

To evaluate the potential benefits of supplementation with the 17 strains, 17-mix or control PBS was orally administered into adult SPF

mice every 2 or 3 days (SPF + 17-mix or SPF + ctrl, respectively). We confirmed a significant increase in the frequency of colonic T_{reg} cells in SPF + 17-mix mice compared with SPF + ctrl mice after 3 weeks of treatment (Fig. 4a). While being continuously treated with 17-mix or control, mice were subjected to the OVA-induced allergic diarrhoea model[19]. The occurrence and severity of diarrhoea and the OVA-specific serum IgE levels were significantly reduced in SPF + 17-mix mice relative to control mice (Fig. 4b–d). The protective effect of 17-mix was significantly attenuated by treatment of mice with a T_{reg}-cell-depleting anti-CD25 antibody (Supplementary Fig. 15). We also subjected mice to an experimental colitis model induced by trinitrobenzene sulphonic acid (TNBS)[20]. SPF + 17-mix mice showed less severe colon shortening and milder histological disease features, accompanied by lower mortality than control mice (Fig. 4e–g and Supplementary Fig. 16a). In keeping with this clinical outcome, there was significantly increased expression of *Foxp3* and *Tgfb1* mRNA in SPF + 17-mix mice compared with control mice, as well as a tendency towards a reduction of inflammatory cytokine transcripts (Supplementary Fig. 16b). Identical suppression of colitis by 17-mix was also observed in an adoptive transfer model, in which germ-free SCID mice were orally inoculated with faeces from SPF mice together with or without 17-mix and then transferred with $CD4^+CD45RB^{hi}$ T cells (Supplementary Fig. 17).

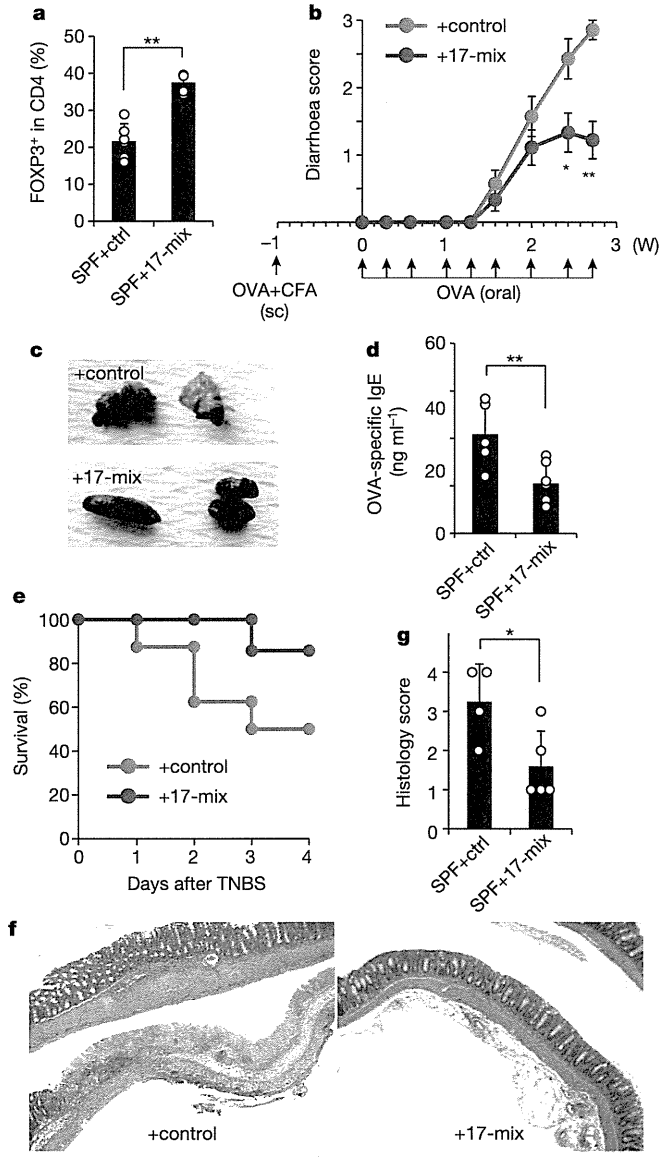

Figure 4 | Treatment with 17-mix suppresses experimental colitis models. **a**, The percentages of $FOXP3^+$ cells within the $CD4^+$ cell population in SPF + 17-mix or SPF + ctrl mice. **b–d**, SPF + 17-mix ($n = 9$) and SPF + ctrl ($n = 7$) mice were subjected to OVA-induced diarrhoea. The diarrhoea score (**b**; see Methods for definition), representative photographs of faeces (**c**), and OVA-specific IgE levels in the sera (**d**) are shown. sc, subcutaneous. **e–g**, SPF + 17-mix ($n = 8$) and SPF + ctrl ($n = 7$) were treated with TNBS. Animal survival (**e**), haematoxylin and eosin staining (original magnification, ×10) (**f**), and histology score of the distal colon (**g**) on day 4 after TNBS administration are shown. Data are representative of two independent experiments. Error bars indicate s.d. $^{**}P < 0.01$; $^{*}P < 0.05$.

The clinical track record of efficacy of single-strain probiotics has been modest. It has been postulated that a collection of functionally distinct bacterial species rationally selected from the human gut microbiota may be more effective than single strains in preventing/treating disease[21]. In the present study, we isolated 17 strains within Clostridia clusters XIVa, IV and XVIII from a human faecal sample; these strains affect T_{reg} cell differentiation, accumulation and function in the mouse colon. It remains to be seen whether the 17 strains will have similar effects in the human intestine; however, a decreased prevalence of Clostridia clusters XIVa and IV in faecal samples from patients with inflammatory bowel disease and atopy[22–24] may suggest that supplementation with the 17-strain bacterial community might counterbalance dysbiosis, induce T_{reg} cells and aid in the management of allergic and inflammatory conditions.

METHODS SUMMARY

Experiments were performed with authorization from the Institutional Review Board for Human Research at RIKEN Yokohama Research Institute. Human stool from a healthy volunteer (Japanese, male, age 31 years) was obtained with informed consent. The sample was mixed with or without chloroform, and the aliquots were inoculated into germ-free IQI mice. Detailed procedures for lamina propria lymphocyte analysis, isolation of bacteria, extraction of bacterial DNA and sequencing are described in Methods. Statistical analysis was performed using the Student's *t*-test.

Full Methods and any associated references are available in the online version of the paper.

Received 14 September 2012; accepted 22 May 2013.
Published online 10 July 2013.

1. Round, J. L. & Mazmanian, S. K. The gut microbiota shapes intestinal immune responses during health and disease. *Nature Rev. Immunol.* **9,** 313–323 (2009).
2. Honda, K. & Littman, D. R. The microbiome in infectious disease and inflammation. *Annu. Rev. Immunol.* **30,** 759–795 (2012).
3. O'Toole, P. W. & Cooney, J. C. Probiotic bacteria influence the composition and function of the intestinal microbiota. *Interdiscip. Perspect. Infect. Dis.* **2008,** 175285 (2008).
4. Atarashi, K. *et al.* Induction of colonic regulatory T cells by indigenous *Clostridium* species. *Science* **331,** 337–341 (2011).
5. Geuking, M. B. *et al.* Intestinal bacterial colonization induces mutualistic regulatory T cell responses. *Immunity* **34,** 794–806 (2011).
6. Russell, S. L. *et al.* Early life antibiotic-driven changes in microbiota enhance susceptibility to allergic asthma. *EMBO Rep.* **13,** 440–447 (2012).
7. Round, J. L. & Mazmanian, S. K. Inducible $Foxp3^+$ regulatory T-cell development by a commensal bacterium of the intestinal microbiota. *Proc. Natl Acad. Sci. USA* **107,** 12204–12209 (2010).
8. Chung, H. *et al.* Gut immune maturation depends on colonization with a host-specific microbiota. *Cell* **149,** 1578–1593 (2012).
9. Sokol, H. *et al. Faecalibacterium prausnitzii* is an anti-inflammatory commensal bacterium identified by gut microbiota analysis of Crohn disease patients. *Proc. Natl Acad. Sci. USA* **105,** 16731–16736 (2008).
10. Thornton, A. M. *et al.* Expression of Helios, an Ikaros transcription factor family member, differentiates thymic-derived from peripherally induced $Foxp3^+$ T regulatory cells. *J. Immunol.* **184,** 3433–3441 (2010).
11. Rubtsov, Y. P. *et al.* Regulatory T cell-derived interleukin-10 limits inflammation at environmental interfaces. *Immunity* **28,** 546–558 (2008).
12. Wing, K. *et al.* CTLA-4 control over $Foxp3^+$ regulatory T cell function. *Science* **322,** 271–275 (2008).
13. Zheng, Y. *et al.* Regulatory T-cell suppressor program co-opts transcription factor IRF4 to control T_H2 responses. *Nature* **458,** 351–356 (2009).
14. Maslowski, K. M. & Mackay, C. R. Diet, gut microbiota and immune responses. *Nature Immunol.* **12,** 5–9 (2011).
15. Lathrop, S. K. *et al.* Peripheral education of the immune system by colonic commensal microbiota. *Nature* **478,** 250–254 (2011).
16. Cebula, A. *et al.* Thymus-derived regulatory T cells contribute to tolerance to commensal microbiota. *Nature* **497,** 258–262 (2013).

17. Collins, M. D. *et al.* The phylogeny of the genus *Clostridium*: proposal of five new genera and eleven new species combinations. *Int. J. Syst. Bacteriol.* **44,** 812–826 (1994).
18. Qin, J. *et al.* A human gut microbial gene catalogue established by metagenomic sequencing. *Nature* **464,** 59–65 (2010).
19. Kweon, M. N., Yamamoto, M., Kajiki, M., Takahashi, I. & Kiyono, H. Systemically derived large intestinal $CD4^+$ Th2 cells play a central role in STAT6-mediated allergic diarrhea. *J. Clin. Invest.* **106,** 199–206 (2000).
20. Strober, W., Fuss, I. J. & Blumberg, R. S. The immunology of mucosal models of inflammation. *Annu. Rev. Immunol.* **20,** 495–549 (2002).
21. Lawley, T. D. *et al.* Targeted restoration of the intestinal microbiota with a simple, defined bacteriotherapy resolves relapsing *Clostridium difficile* disease in mice. *PLoS Pathog.* **8,** e1002995 (2012).
22. Frank, D. N. *et al.* Molecular-phylogenetic characterization of microbial community imbalances in human inflammatory bowel diseases. *Proc. Natl Acad. Sci. USA* **104,** 13780–13785 (2007).
23. Manichanh, C. *et al.* Reduced diversity of faecal microbiota in Crohn's disease revealed by a metagenomic approach. *Gut* **55,** 205–211 (2006).
24. Candela, M. *et al.* Unbalance of intestinal microbiota in atopic children. *BMC Microbiol.* **12,** 95 (2012).

Supplementary Information is available in the online version of the paper.

Acknowledgements This work was supported by JSPS NEXT program, Grant in Aid for Scientific Research on Innovative Areas 'Genome Science' from the Ministry of Education, Culture, Sports, Science and Technology of Japan (No.221S0002), the global COE project of 'Genome Information Big Bang' and the Waksman Foundation of Japan Inc. We thank M. Suyama, K. Furuya, C. Yoshino, H. Inaba, E. Iioka, Y. Takayama, M. Kiuchi, Y. Hattori, N. Fukuda and A. Nakano for technical assistance, and P. D. Burrows for review of the manuscript.

Author Contributions K.Ho. planned experiments, analysed data and wrote the paper together with B.O. and M.H.; K.A. and T.Tano. performed immunological analyses and bacterial cultures together with Y.N., S.N. and H.M.; W.S., K.O., S.K. and M.H. performed bacterial sequence analyses; K.M. and S.U. provided essential materials; H.N., T.S. and S.S. supervised the T_{reg} cell suppression assay; S.F., K.Ha., H.O., T.Tani., J.V.F. and P.W. were involved in data discussions.

Author Information All genome sequence data are deposited in DDBJ BioProject ID PRJDB521-543. Reprints and permissions information is available at www.nature.com/reprints. The authors declare competing financial interests: details are available in the online version of the paper. Readers are welcome to comment on the online version of the paper. Correspondence and requests for materials should be addressed to M.H. (hattori@k.u-tokyo.ac.jp) or K.Ho. (kenya@rcai.riken.jp).

METHODS

Mice and rats. C57BL/6, BALB/c, IQI/Jic and CB.17 SCID mice and F344 rats kept under SPF or germ-free conditions were purchased from Sankyo laboratories, Japan SLC, or CLEA Japan. IQI germ-free mice were used unless otherwise indicated. Germ-free and gnotobiotic mice were bred and maintained in vinyl isolators within the gnotobiotic facility of Sankyo laboratories. Germ-free *Il10*^{Venus} mice were generated as previously described[4]. OT-I and OT-II T-cell receptor transgenic mice were purchased from Taconic Farms. All animal experiments were approved by the Animal Research Committee of RIKEN Yokohama Institute and the University of Tokyo.

Chloroform treatment of human stool and generation of gnotobiotic mice. Human stool from a healthy volunteer (Japanese, male, age 31 years) was obtained with informed consent. Human stool and mouse caecal contents were directly frozen at −80 °C, or suspended in 4 times volume (w/v) of phosphate-buffered saline (PBS) + 20% glycerol solution, snap-frozen in liquid nitrogen and stored at −80 °C until use. The frozen stocks were thawed, suspended in 10 times volume (w/v) of PBS, and passed through a 70 μm cell strainer to eliminate clumps and debris. Then suspensions were mixed with chloroform (final concentration 3%), and incubated in a shaking water bath for 60 min. After evaporation of chloroform by bubbling with N_2 gas for 30 min, the aliquots containing the chloroform-resistant fraction of intestinal bacteria were inoculated into germ-free mice by intra-gastric administration (250 μl; per mouse). To generate a series of gnotobiotic mice inoculated with diluted samples, caecal contents from exGF mice were treated with chloroform, diluted with PBS, and inoculated into germ-free IQI mice. The caecal suspensions diluted 2×10^4-fold correspond to 2.5×10^4 bacterial cells per mouse. Each group of exGF mice was individually caged in the gnotobiotic isolator for 3–4 weeks at Sankyo Lab service.

Isolation of intestinal lamina propria lymphocytes and flow cytometry. The colons were collected and opened longitudinally, washed with PBS to remove all luminal contents and shaken in Hanks' balanced salt solution (HBSS) containing 5 mM EDTA for 20 min at 37 °C. After removing epithelial cells, muscle layers and fat tissue using forceps, the lamina propria layers were cut into small pieces and incubated with RPMI1640 containing 4% fetal bovine serum, 0.5 mg ml^{-1} collagenase D, 0.5 mg ml^{-1} dispase and 40 μg ml^{-1} DNase I (all Roche Diagnostics) for 1 h at 37 °C in a shaking water bath. The digested tissues were washed with HBSS containing 5 mM EDTA, resuspended in 5 ml of 40% Percoll (GE Healthcare) and overlaid on 2.5 ml of 80% Percoll in a 15-ml Falcon tube. Percoll gradient separation was performed by centrifugation at 800*g* for 20 min at 25 °C. The lamina propria lymphocytes were collected from the interface of the Percoll gradient and suspended in ice-cold PBS. For analysis of T_{reg} cells, isolated lymphocytes were labelled with the LIVE/DEAD fixable dead cell stain kit (Invitrogen) to exclude dead cells from the analysis. The cells were washed with staining buffer containing PBS, 2% FBS, 2 mM EDTA and 0.09% NaN_3 and surface staining was performed with PECy7- or Pacific blue-labelled anti-CD4 antibody (RM4-5, BD Biosciences), PE-labelled anti-ICOS antibody (C938.4A, BioLegend), Alexa488-labelled anti-CD103 antibody (2E7, BioLegend), and PerCP/Cy5.5-labelled anti-integrin-β7 antibody (FIB27, BioLegend). Intracellular staining of FOXP3, CTLA4, Helios and Ki67 was performed using the Alexa647-labelled anti-FOXP3 antibody (FJK-16 s, eBioscience), PE-labelled anti-CTLA4 antibody (UC10-4F10-11, BD Biosciences), PE-labelled anti-Helios antibody (22F6, BioLegend), PECy7-labelled anti-Ki67 antibody (B56, BD Biosciences) and FOXP3 staining buffer set (eBioscience). For analysis of T_H1 and T_H17 cells, isolated lymphocytes were stimulated for 4 h with 50 ng ml^{-1} phorbol 12-myristate 13-acetate (PMA, Sigma) and 1 μg ml^{-1} ionomycin (Sigma) in the presence of GolgiStop (BD Biosciences). After incubation for 4 h, cells were washed in PBS, labelled with the LIVE/DEAD fixable dead cell stain kit and surface CD4 was stained with PECy7-labelled anti-CD4 antibody. Cells were washed, fixed in Cytofix/Cytoperm, permeabilized with Perm/Wash buffer (BD Biosciences), and stained with the APC-labelled anti-IL-17 antibody (eBio17B7, eBioscience) and FITC-labelled anti-IFN-γ antibody (XMG1.2, BD Biosciences). The antibody-stained cells were analysed with LSR Fortessa or FACSAriaIII (BD Biosciences), and data were analysed using FlowJo software (Treestar).

Meta 16S rRNA gene sequencing. The caecal contents from exGF mice were suspended in 10 ml of Tris-EDTA containing 10 mM Tris-HCl and 1 mM EDTA (pH 8), and incubated with lysozyme (Sigma, 15 mg ml^{-1}) at 37 °C for 1 h with gentle mixing. A purified achromopeptidase (Wako) was added (final concentration 2,000 unit ml^{-1}) and further incubated at 37 °C for another 30 min. Then, sodium dodecyl sulphate (final concentration 1%) was added to the cell suspension and mixed well. Subsequently, proteinase K (Merck) was added (final concentration 1 mg ml^{-1}) to the suspension and the mixture was incubated at 55 °C for 1 h. High-molecular-mass DNA was isolated and purified by phenol/chloroform extraction, ethanol and finally polyethyleneglycol precipitation[25]. PCR was performed using Ex Taq (TAKARA) and (1) the 454 primer A (5′-CCATCTCA TCCCTGCGTGTCTCCGACTCAG (454 adaptor sequence) + barcode (10 bases) + AGRGTTTGATYMTGGCTCAG-3′ (27Fmod)) and (2) the 454 primer B (5′-CCTATCCCCTGTGTGCCTTGGCAGTCTCAG (454 adaptor sequence) + TGCTGCCTCCCGTAGGAGT-3′ (338R)) to the V1–V2 region of the 16S rRNA gene. Amplicons generated from each sample (~330 bp) were subsequently purified using AMPur XP (Beckman Coulter). The amount of DNA was quantified using Quant-iT Picogreen dsDNA assay kit (Invitrogen) and TBS-380mini fluorometer (Turner Biosystems). Then, the amplified DNA was used as template for 454 GS Junior (Roche) pyrosequencing using GS Junior Titanium emPCR Kit-Lib-L, GS Junior Titanium Sequencing Kit and GS Junior Titanium PicoTiterPlate Kit (all Roche) according to the manufacturer's instructions. Quality-filter-passed reads were obtained by removing reads that did not have both primer sequences, had the average quality value (QV) <25, and were possibly chimaeric[26]. Of the filter-passed reads, 3,000 reads trimming off both primer sequences for each sample were used and subjected to OTU analysis with the cutoff similarity of 96% identity. Representative sequences from each OTU were blasted to Ribosomal Database Project (RDP) of bacterial isolates, our genome database constructed from publically available genome sequences in NCBI and HMP databases, and 16S sequences of the 23 strains obtained in this study.

Isolation of bacterial strains. The frozen stocks of caecal contents from exGF mice were serially diluted with PBS and seeded onto non-selective agar plates (blood liver (BL) agar (Eiken Chemical) or Eggerth-Gagnon (EG) agar plates). EG agar plates contain the following components (quantities expressed per litre): Lab-Lemco Powder (2.8 g, Oxoid); proteose peptone no. 3 (10.0 g, Difco); yeast extract (5.0 g, Difco); Na_2HPO_4 (4.0 g); D(+)-glucose (1.5 g); soluble starch (0.5 g); L-cystine (0.2 g); L-cysteine-HCl-H_2O (0.5 g); Tween 80 (0.5 g); Bacto agar (16.0 g, Difco); and defibrinated horse blood (50 ml). After culture under aerobic conditions or strictly anaerobic conditions (80% N_2, 10% H_2, 10% CO_2) at 37 °C for 2 or 4 days, individual colonies were picked up and cultured for an additional 2 or 4 days at 37 °C in ABCM broth (Eiken Chemical) or EG agar plate. The isolated strains were collected into EG stock medium (10% glycerol) and stored at −80 °C. To identify the isolated strains, 16S rRNA gene sequences were determined. The 16S rRNA gene was amplified by colony-PCR using KOD FX (TOYOBO) and GeneAmp PCR System9700 (Applied Biosystems) using 16S rRNA gene-specific primer pairs: 8F (5′-AGAGTTTGATCMTGGCTCAG-3′) and 519R (5′-ATTACCGCGGCKGCTG-3′) or 1513R (5′-ACGGCTACCTTGTTACGACTT-3′). The amplification program consisted of one cycle at 98 °C for 2 min, followed by 40 cycles at 98 °C for 10 s, 57 °C for 30 s and 68 °C for 1 min 30 s. Each amplified DNA was purified from the reaction mixture using Illustra GFX PCR DNA and gel band purification kit (GE Healthcare). Sequence analysis was performed using BigDye Terminator V3.1 cycle sequencing kit (Applied Biosystems) and Applied Biosystems 3730xl DNA analyser (Applied Biosystems). The resulting sequences were compared with sequences in RDP database and genome database using BLAST to determine close species/strains.

Bacterial culture of isolated strains. The isolated strains of Clostridia and Erysipelotrichi were cultured in EG broth without horse blood under a strictly anaerobic condition (80% N_2, 10% H_2, 10% CO_2) at 37 °C in an anaerobic chamber (Coy Laboratory Products). To prepare the bacterial mixture, bacterial strains were individually grown in EG broth to confluence and mixed at equal amounts of media volume.

Scanning electron microscopy. Scanning electron microscopy was performed by Filgen, Inc., Japan. The proximal colon was removed from +23-mix mice, cut open longitudinally, prefixed with 2% glutaraldehyde in 0.1 M phosphate buffer (pH 7.4) for 24 h at 4 °C, and then postfixed with 2% osmium tetroxide for 1 h at 4 °C. Fixed samples were dehydrated for 5 min each in sequential baths of 50%, 70%, 90% and 100% ethanol, inserted into a critical point dryer until dry and coated with osmium in an OPC-80N osmium plasma coater (Filgen). Scanning electron micrographs were taken by a JEOL JSM-6320F instrument.

Measurement of organic acids. Organic acid concentrations in caecal contents were determined by gas chromatography-mass spectrometry (GC-MS). Caecal contents (10 mg) were disrupted using 3-mm zirconia/silica beads (BioSpec Products) and homogenized in extraction solution containing 100 μl of internal standard (100 μM crotonic acid), 50 μl of HCl and 200 μl of ether. After vigorous shaking using a Shakemaster neo (Bio Medical Science) at 1,500 r.p.m. for 10 min, homogenates were centrifuged at 1,000*g* for 10 min and then the top ether layer was collected and transferred into new glass vials. Aliquots (80 μl) of the ether extracts were mixed with 16 μl of *N*-tert-butyldimethylsilyl-*N*-methyltrifluoroacetamide (MTBSTFA). The vials were sealed tightly by screwing and heated at 80 °C for 20 min in a water bath, and left at room temperature for 48 h for derivatization. The derivatized samples were run through a 6890N Network GC System (Agilent Technologies) equipped with HP-5MS column (0.25 mm × 30 m × 0.25 μm) and 5973 Network Mass Selective Detector (Agilent Technologies). Pure helium (99.9999%) was used as a carrier gas and delivered at a flow rate of 1.2 ml min^{-1}.

The head pressure was set at 10 p.s.i. with split 10:1. The inlet and transfer line temperatures were 250 °C and 260 °C, respectively. The following temperature program was used: 60 °C (3 min), 60–120 °C (5 °C min^{-1}), 120–300 °C (20 °C min^{-1}). One microlitre quantity of each sample was injected with a run time of 30 min. Organic acid concentrations were quantified by comparing their peak areas with the standards.

Genome sequencing and gene prediction. The genome sequences of 17 T_{reg}-cell-inducing strains were determined by the whole-genome shotgun strategy using a 454GS FLX Ti or Ion PGM sequencer. Each 1–5 μg of the genomic DNA was sheared to obtain DNA fragments. Template DNA was prepared according to the supplier's protocol. The generated sequence data were assembled using Newbler v2.8 software to obtain the draft genome sequences. All genome sequence data were deposited in DDBJ BioProject ID: PRJDB521-543. Protein-encoding genes were predicted using MetaGeneAnnotator software[27]. Putative toxins and virulence factors were searched using the BLASTP program and virulence factor databases, VFDB (http://www.mgc.ac.cn/VFs/main.htm) and MvirDB (http://mvirdb.llnl.gov), with the *e*-value cutoff of 1.0×10^{-10}, the identity >30% and the length coverage >60%.

Phylogenetic tree. Sequences concatenated with genes encoding 26 ribosomal proteins (large subunit L10, L11, L14, L16, L17, L19, L20, L23, L24, L29, L31, L32, L35, L7/L12, and small subunit S10, S12, S13, S15, S16, S17, S20, S20, S21, S3, S4, S7, S8) predicted from the genomes of each strain were used to construct a phylogenetic tree. The sequences of other bacterial species used for the tree construction were obtained from the ribosomal multi-locus sequencing typing (MLST) database[28]. The calculation was performed using the MEGA v5.0 package and the neighbour-joining method with a bootstrap of 1,000 replicates.

Cognate antigen-driven T_{reg} cell suppression assay. Preparation of antigens in caecal contents was performed as previously reported[15]. Caecal contents from germ-free mice or +17-mix mice were collected and suspended in PBS (500 mg ml^{-1}); they were then filtered through a 70-μm mesh, and autoclaved at 121 °C for 15 min. To prepare antigens of bacterial components, the 17 strains of Clostridia were cultured *in vitro*, mixed, washed and suspended with 1 ml PBS, and autoclaved at 121 °C for 20 min. $CD11c^+$ cells were isolated by FACSAriaIII from spleens of SPF C57BL/6 mice and pulsed for 1 h with 0.5 μM SIINFEKL OT-I peptide alone or in combination with either of 5 μM ISQAVHAAHAEINEAGR OT-II peptide, autoclaved caecal contents from +17-mix mice or germ-free mice (diluted 1:200), or autoclaved 17 strains of bacteria cultured *in vitro* (diluted 1:200). The antigen-pulsed $CD11c^+$ cells were plated at 5×10^4 per well in 96-well round-bottomed plates. CD8 T cells (T_{eff} cells) were sorted from spleens of SPF OT-I mice by FACSAriaIII and added to the $CD11c^+$ cell-seeded plates at 5×10^4 per well. Then, $CD4^+CD25^+$ T cells (T_{reg} cells) sorted from colonic lamina propria of +17-mix mice or from spleens of SPF OT-II mice were added to the culture at the indicated ratio of T_{reg} to T_{eff} cells. After 3 days, all cells were harvested, stained with anti-CD4 and anti-CD8 antibodies, and analysed by FACSAriaIII to enumerate the number of CD8 OT-I T cells.

Intestinal epithelial cell stimulation with caecal extracts and SCFAs. To prepare caecal extracts, frozen caecal contents from germ-free, +17-mix or SPF mice were thawed and well suspended in 4 volumes of sterile water. After centrifugation (5,000 r.p.m. for 15 min), transparent supernatants were collected, filtered through 0.22 μm filter and used as caecal extracts. In some experiments, caecal extracts were treated with proteinase K (2 mg ml^{-1}, 55 °C for 1 h; Roche) or nuclease that degrades all forms of DNA and RNA (125 unit ml^{-1}, 37 °C for 4 h; Thermo), and subsequently heated at 95 °C for 5 min to inactivate the enzymes. Human intestinal epithelial cell lines (HCT8, HT29, Caco2, T84 and Colo205) and a mouse epithelial cell line (CMT93) were obtained from ATCC and maintained at 37 °C (5% CO2) in RPMI containing 10% heat-inactivated horse serum (Invitrogen). Cells were cultured at 1.5×10^5 cells in 150 μl medium in 48-well plates and stimulated with 4.5 μl caecal extract for 24 h. Human primary intestinal epithelial cells were obtained from Lonza and maintained at 33 °C (5% CO2) in SmGM-2 medium containing 10% FBS (Lonza) for 1–2 weeks (6×10^4 cells in 48-well plates). The medium was changed to 150 μl SmGM-2 containing 1% FBS before stimulation. Caecal extracts (4.5 μl) were added to the culture and incubated for 24 h. Culture supernatants were collected and the level of the active form of TGF-β1 (Promega), TNF-α (R&D) and IL-6 (R&D) was measured by ELISA. To stimulate epithelial cell lines with SCFAs, sodium salts of acetate, butyrate, propionate and isobutyrate were dissolved in PBS. SCFAs were added to the culture individually (final 0.5 mM) or in combination (final 0.5 mM each), and incubated for 24 h.

TNBS colitis. C57BL/6 SPF adult mice were orally inoculated with 17-mix or control PBS every 2 or 3 days for 3 weeks. 2,4,6-Trinitrobenzene sulphonic acid (TNBS)-induced colitis was induced by the intracolonic administration of 2.5 mg of TNBS (Sigma) in 50% ethanol into anaesthetized mice via a thin round-tip needle. The tip of the needle was inserted 4 cm proximal to the anal verge, and mice were held in a vertical position for 30 s after the injection. All the mice were observed daily and were killed on day 4 after TNBS administration. Colons were fixed with 4% paraformaldehyde, sectioned, and stained with haematoxylin and eosin. The degree of inflammation in the distal part of colon was graded from 0 to 4 as follows: 0, normal; 1, ulcer with cell infiltration limited to the mucosa; 2, ulcer with limited cell infiltration in the submucosa; 3, focal ulcer involving all layers of the colon; 4, multiple lesions involving all layers of the colon, or necrotizing ulcer larger than 1 mm in length.

Allergic diarrhoea. BALB/c SPF adult mice were primed by subcutaneous injection with 1 mg of OVA (Fraction V; Sigma) in 100 μl of Complete Freund Adjuvant (CFA, DIFCO). One week after priming, mice were given 50 mg of OVA dissolved in 200 μl of PBS by intra-gastric administration three times per week. 17-mix or control PBS was orally administered to mice every 2 or 3 days for the entire period of the experiments. Diarrhoea was monitored visually 1 h after each oral OVA challenge. Diarrhoea was scored as follows: 0, normal faeces (solid); 1, moist faeces (semi-solid); 2, mild diarrhoea (loose); and 3, severe diarrhoea (watery). Serum was collected from the cheek vein 1 h after the last OVA challenge and OVA-specific IgE levels were measured by ELISA (Chondrex).

Adoptive $CD4^+CD45RB^{hi}$ T-cell transfer model of colitis. Germ-free CB.17 SCID mice were orally inoculated with SPF faeces together with or without 17-mix of Clostridia. One week later, exGF SCID mice received 4×10^5 $CD4^+CD45RB^{hi}$ T cells by intraperitoneal injection. Naive $CD4^+CD45RB^{hi}$ T cells were isolated from spleens of SPF BALB/c mice by FACS sorting. All the mice were observed daily and were killed on day 14 after T-cell transfer.

25. Morita, H. *et al.* An improved isolation method for metagenomic analysis of the microbial flora of the human intestine. *Microbes Environ.* **22,** 214–222 (2007).
26. Kim, S. W. *et al.* Robustness of gut microbiota of healthy adults in response to probiotic intervention revealed by high-throughput pyrosequencing. *DNA Res.* **20,** 241–253 (2013).
27. Noguchi, H., Taniguchi, T. & Itoh, T. MetaGeneAnnotator: detecting species-specific patterns of ribosomal binding site for precise gene prediction in anonymous prokaryotic and phage genomes. *DNA Res.* **15,** 387–396 (2008).
28. Jolley, K. A. *et al.* Ribosomal multilocus sequence typing: universal characterization of bacteria from domain to strain. *Microbiology* **158,** 1005–1015 (2012).

European Journal of Immunology

Overcoming regulatory T-cell suppression by a lyophilized preparation of *Streptococcus pyogenes*

Michiko Hirayama[*1,2], *Hiroyoshi Nishikawa*[*1,3], *Yasuhiro Nagata*[4], *Takemasa Tsuji*[5], *Takuma Kato*[6], *Shinichi Kageyama*[2], *Shugo Ueda*[7], *Daisuke Sugiyama*[3], *Sahoko Hori*[1,2], *Shimon Sakaguchi*[3], *Gerd Ritter*[5], *Lloyd J. Old*[5], *Sacha Gnjatic*[5] *and Hiroshi Shiku*[1,2]

[1] Department of Cancer Vaccine, Mie University Graduate School of Medicine, Mie, Japan
[2] Department of Immuno-Gene Therapy, Mie University Graduate School of Medicine, Mie, Japan
[3] Experimental Immunology, Immunology Frontier Research Center, Osaka University, Osaka, Japan
[4] Department of Surgery, National Hospital Organization Nagasaki Medical Center, Nagasaki, Japan
[5] Ludwig Institute for Cancer Research, New York Branch, Memorial Sloan-Kettering Cancer Center, New York, NY, USA
[6] Department of Cellular and Molecular Immunology, Mie University Graduate School of Medicine, Mie, Japan
[7] Department of Gastroenterological Surgery and Oncology, Kitano Hospital, Tazuke Kofukai Medical Research Institute, Osaka, Japan

Cancer vaccines have yet to yield clinical benefit, despite the measurable induction of humoral and cellular immune responses. As immunosuppression by $CD4^+CD25^+$ regulatory T (Treg) cells has been linked to the failure of cancer immunotherapy, blocking suppression is therefore critical for successful clinical strategies. Here, we addressed whether a lyophilized preparation of *Streptococcus pyogenes* (OK-432), which stimulates Toll-like receptors, could overcome Treg-cell suppression of $CD4^+$ T-cell responses in vitro and in vivo. OK-432 significantly enhanced in vitro proliferation of $CD4^+$ effector T cells by blocking Treg-cell suppression and this blocking effect depended on IL-12 derived from antigen-presenting cells. Direct administration of OK-432 into tumor-associated exudate fluids resulted in a reduction of the frequency and suppressive function of $CD4^+CD25^+Foxp3^+$ Treg cells. Furthermore, when OK-432 was used as an adjuvant of vaccination with HER2 and NY-ESO-1 for esophageal cancer patients, NY-ESO-1–specific $CD4^+$ T-cell precursors were activated, and NY-ESO-1–specific $CD4^+$ T cells were detected within the effector/memory T-cell population. $CD4^+$ T-cell clones from these patients had high-affinity TCRs and recognized naturally processed NY-ESO-1 protein presented by dendritic cells. OK-432 therefore inhibits Treg-cell function and contributes to the activation of high-avidity tumor antigen-specific naive T-cell precursors.

Keywords: Cancer · Treg cells · Tumor immunology · Vaccination

Additional supporting information may be found in the online version of this article at the publisher's web-site

Correspondence: Dr. Hiroyoshi Nishikawa
e-mail: nisihiro@ifrec.osaka-u.ac.jp

*These authors contributed equally to this work.

Introduction

Many tumor-associated antigens recognized by the immune system are normal self-constituents, and tumor immunity is considered to be in part an autoimmune response [1–3]. Therefore, mechanisms for maintaining immunological self-tolerance hamper effective anticancer immunity. $CD4^+CD25^+$ Treg cells are one of the major components in maintaining immunological self-tolerance in hosts by suppressing a wide range of immune responses [4–7]. Indeed, depletion of Treg-cell populations enhances spontaneous and vaccine-induced antitumor immune responses [6, 8, 9], and the stimulation of $CD4^+CD25^+$ Treg cells by immunization with self-antigens induces enhanced chemically induced primary tumor development and increased numbers of pulmonary metastasis following injection of transplantable tumor cells [10–12]. In human cancers, the presence of high numbers of $CD4^+CD25^+$ Treg cells or low ratio of $CD8^+$ T cells to $CD4^+CD25^+$ Treg cells in tumors is correlated with unfavorable prognosis [13, 14]. In addition, the depletion of $CD4^+CD25^+$ Treg cells in patients receiving a DC vaccine enhances the stimulation of tumor-specific T-cell responses, indicating a crucial role for Treg cells in the regulation of antitumor immune responses in humans [15].

NY-ESO-1, a germ cell protein, was found by SEREX (serological identification of antigens by recombinant expression cloning) using the serum of an esophageal cancer patient [16, 17]. We have previously shown that NY-ESO-1–specific $CD4^+$ T cells are detectable in cancer patients with spontaneous NY-ESO-1 serum Ab responses [17, 18]. In addition, NY-ESO-1–specific $CD4^+$ T-cell precursors can expand and become detectable in healthy individuals after in vitro antigenic stimulation of peripheral $CD4^+$ T cells, but only following depletion of $CD4^+CD25^+$ T cells [19, 20]. These results suggested that NY-ESO-1–specific $CD4^+$ T-cell precursors are actually present at relatively high frequencies in healthy individuals, and that the activation/expansion of NY-ESO-1–specific naive $CD4^+$ T cells is suppressed by $CD4^+CD25^+$ Treg cells. In healthy donors and in cancer patients with NY-ESO-1–expressing tumors but without spontaneous anti-NY-ESO-1 Ab (seronegative), naturally arising NY-ESO-1–specific T-cell responses are susceptible to Treg-cell suppression and are exclusively detected from naive populations ($CD4^+CD25^-CD45RA^+$). In contrast, most NY-ESO-1–specific $CD4^+$ T cells in cancer patients with spontaneous anti-NY-ESO-1 Ab (seropositive) are derived from memory populations ($CD4^+CD25^-CD45RO^+$) and are detectable even in the presence of $CD4^+CD25^+$ Treg cells [20, 21]. After vaccination with HLA-DPB1*0401/0402-restricted NY-ESO-$1_{157-170}$ peptide in incomplete Freund's adjuvant, ovarian cancer patients develop NY-ESO-1–specific $CD4^+$ T cells with only low avidity to antigen and low sensitivity to Treg cells, even though they have an effector/memory phenotype ($CD4^+CD25^-CD45RO^+$) [21]. Still, high-avidity naive NY-ESO-1–specific T-cell precursors are present in the peripheral blood of vaccinated patients, but they are subjected to continuous $CD4^+CD25^+$ Treg-cell suppression throughout vaccination [21]. Thus, a strategy to overcome Treg-cell suppression on preexisting high-avidity naive T-cell precursors is an essential component for effective cancer vaccines.

Accumulating data shed light on recognition of pathogen-associated molecular patterns through TLRs to break the suppressive environment in tumors [22]. It has been reported that TLR stimulants, such as lipopolysaccharide or CpG, block the suppressive activity of $CD4^+CD25^+$ Treg cells partially by an IL-6–dependent mechanism [23]. TLR2 signaling was reported to stimulate the proliferation of $CD4^+CD25^+$ Treg cells and to induce temporal loss of suppressive activity of $CD4^+CD25^+$ Treg cells [24]. TLR2 signaling has also been shown to increase IL-2 secretion by effector T cells, thereby rendering them resistant to $CD4^+CD25^+$ Treg-cell–mediated suppression [25]. We and others have recently reported that vaccination of tumor antigens by TLR stimulating viral or bacterial vectors was able to not only inhibit the suppressive function of $CD4^+CD25^+$ Treg cells but also break tolerance or hyporesponsiveness of effector T cells to tumor antigens even in the presence of Treg cells [26–28].

OK-432 is a lyophilized preparation of *Streptococcus pyogenes* that binds TLR-2, TLR-4, and/or TLR-9 and activates APCs, making it attractive for potential use as an adjuvant of cancer vaccine [29–33]. OK-432–matured DCs effectively prime antigen-specific T cells in vitro [29, 34]. Importantly, OK-432 has already been used for many years as a direct anticancer agent, particularly in Japan, and has a well-established clinical safety profile. However, while it is considered that OK-432 may inhibit Treg-cell suppressive activity by stimulating several TLR signaling pathways, its influence on Treg cells has not yet been shown. In this study, we addressed whether OK-432 inhibits Treg-cell suppressive function and could be a promising adjuvant of cancer vaccines.

Results

OK-432 inhibits the suppressive activity of $CD4^+CD25^+$ Treg cells

To address whether OK-432 inhibited $CD4^+CD25^+$ Treg-cell suppression, we employed the standard in vitro suppression system. $CD4^+CD25^-$ T cells and $CD4^+CD25^{high}$ Treg cells (highest 3% of $CD4^+CD25^+$ cells) were isolated from PBMCs of healthy individuals. $CD4^+CD25^-$ T cells were cultured with irradiated autologous APCs (CD4-depleted PBMCs) and anti-CD3 Ab in the presence or absence of $CD4^+CD25^{high}$ Treg cells. $CD4^+CD25^-$ T-cell proliferation was analyzed as described in the *Materials and methods*. In accordance with previous reports [7], $CD4^+CD25^{high}$ Treg cells markedly suppressed the proliferation of $CD4^+CD25^-$ T cells (Fig. 1A and B). In sharp contrast, when OK-432 was added in the culture, suppressive activity of $CD4^+CD25^{high}$ T cells was significantly inhibited (Fig. 1A and B). In addition, OK-432 did not induce death of $CD4^+CD25^{high}$ Treg cells as the frequency of Annexin V^+ and 7-AAD^+ cells was not significantly increased in the presence of OK-432 (data not shown). Instead, $CD4^+CD25^{high}$ Treg cells exhibited marginal proliferation in the presence of

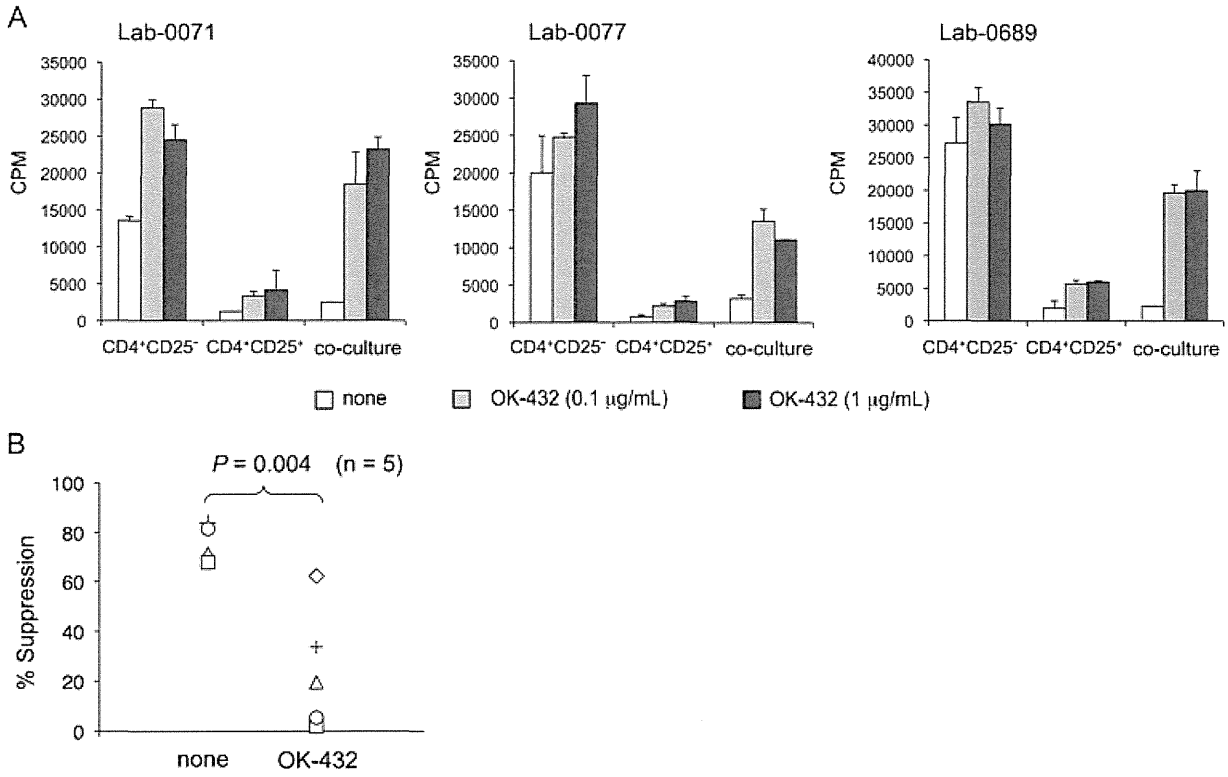

Figure 1. OK-432 overcomes Treg-cell suppression in vitro. (A, B) $CD4^+CD25^-$ T cells and $CD4^+CD25^{high}$ Treg cells were collected from PBMCs of healthy individuals as described in the *Materials and Methods*. 1×10^4 $CD4^+CD25^-$ T cells were cultured with irradiated autologous CD4-depleted PBMCs and anti-CD3 Ab in the presence or absence of 5×10^3 $CD4^+CD25^+$ Treg cells with/without OK-432. Proliferation was analyzed by ^3H-thymidine incorporation. Data of three donors are shown as mean + SD of two replicates/samples and are from one experiment representative of at least two performed. (B) Summary of percent suppression in five healthy individuals. Percent suppression was calculated as: (1 – (cpm in coculture)/(cpm in $CD4^+CD25^-$ T cells)) × 100. Data shown are from one experiment representative of at least two performed.

OK-432 (Fig. 1A). These data indicate that addition of OK-432 impairs the suppressive activity of $CD4^+CD25^{high}$ Treg cells and partially reverses anergy status of Treg cells.

Inhibition of the suppressive activity of $CD4^+CD25^+$ Treg cells by OK-432 is dependent on IL-12

Since OK-432 reportedly induces TLR-2, TLR-4, and/or TLR-9 activation and subsequent production of proinflammatory cytokines [29–33], we examined the involvement of cytokines in this inhibition of Treg-cell suppression. To this end, Abs against several candidate cytokines were added to cultures. Among cytokines tested, only blocking Ab against IL-12 significantly abrogated the inhibition of Treg-cell suppression by OK-432 (Fig. 2A).

To confirm the importance of IL-12, we next analyzed whether the addition of IL-12 could inhibit Treg-cell suppression as observed by OK-432. $CD4^+CD25^-$ T cells were cultured with $CD4^+CD25^{high}$ Treg cells, irradiated autologous APCs and anti-CD3 Ab in the presence of IL-12. Treg-cell suppressive activity was significantly inhibited by the addition of IL-12, but not IL-6 or IFN-γ (Fig. 2B). Again, IL-12 did not kill $CD4^+CD25^{high}$ Treg cells as the frequency of Annexin V^+ and 7-AAD^+ cells was not significantly increased in the presence of IL-12 (data not shown). Instead, $CD4^+CD25^{high}$ Treg cells slightly proliferated in the presence of OK-432 (Fig. 2B). These data suggest a critical role for IL-12 in the inhibition of Treg-cell suppression by OK-432.

OK-432 induces higher amounts of IL-12 but not IL-10 from APCs compared with other stimuli

To gain insight into the cellular target(s) of OK-432, we explored the origin of IL-12 after OK-432 treatment based on the essential role of IL-12 in the inhibition of Treg-cell suppression by OK-432. We then analyzed whether OK-432 stimulation indeed induced IL-12 production from APCs, such as CD3-depleted PBMCs used in the standard Treg-cell suppression assays. CD3-depleted PBMCs from healthy donors were stimulated with OK-432, LPS, or TNF-α, and cytokine production was examined. OK-432 induced significantly higher amounts of IL-12 from CD3-depleted PBMCs than LPS or TNF-α (Fig. 3A). In addition, CD3-depleted PBMCs stimulated with OK-432 induced much less IL-10 production than LPS (Fig. 3A). Similar results, i.e. IL-12 rather than IL-10 was dominantly produced by CD3-depleted PBMCs stimulated with OK-432, were obtained from four esophageal cancer patients (Fig. 3B).

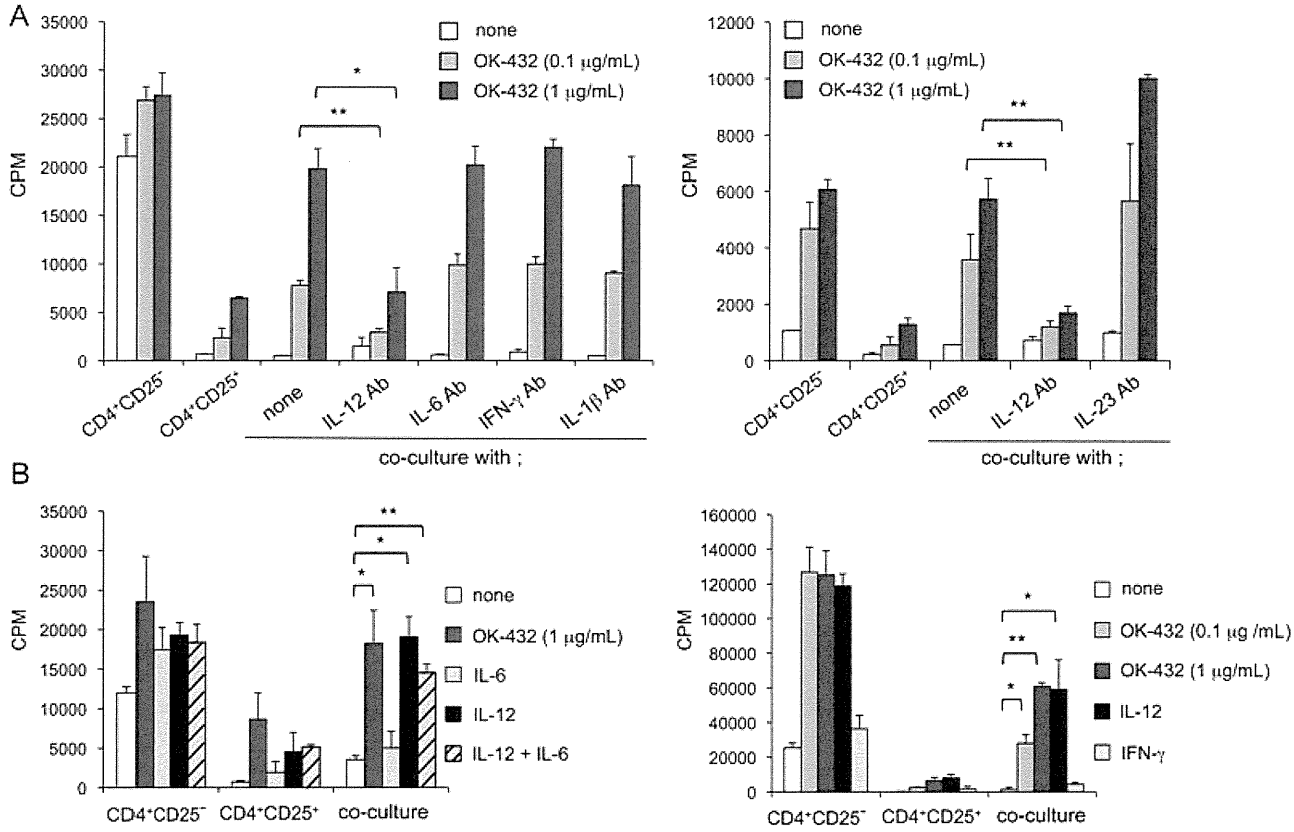

Figure 2. IL-12 is a critical cytokine to overcome Treg-cell suppression by OK-432. $CD4^+CD25^-$ T cells and $CD4^+CD25^{high}$ Treg cells were collected from PBMCs of healthy individuals. 1×10^4 $CD4^+CD25^-$ T cells were cultured with 1×10^5 irradiated autologous CD4-depleted PBMCs and anti-CD3 Ab in the presence or absence of 2.5×10^3 $CD4^+CD25^{high}$ Treg cells with/without OK-432. (A) Blocking Abs (10 μg/mL) against several cytokines as indicated were added in the culture and proliferation was measured. (B) Recombinant cytokines (IL-12; 5 ng/mL, IL-6; 5 ng/mL, IFN-γ; 100 U/mL) were added into the cultures and proliferation was analyzed. Data for one representative donor among three donors are expressed as mean + SD of two replicates/samples and are from one experiment representative of at least two performed. $^*p < 0.05$ and $^{**}p < 0.01$ as compared with control, Student's t-test.

We next examined which cell types in PBMCs produced IL-12 after OK-432 stimulation. The major sources of IL-12 in PBMCs after OK-432 stimulation were $CD11c^+$ and $CD14^+$ cells, and neither NK cells nor T cells produced IL-12 (Fig. 3C). Taken together, APCs, such as monocytes, macrophages, and DCs are considered to be the cellular targets of OK-432 to induce IL-12 which is a crucial component for the inhibition of Treg-cell suppression by OK-432.

OK-432 administration to tumor-associated exudates reduces local Treg-cell accumulation and function

As OK-432 is available as an anticancer agent in Japan and has been used for controlling tumor-associated exudate fluids by direct injection to the cavity, we next investigated its influence on Treg cells following in vivo treatment of OK-432. We analyzed the local Treg-cell accumulation and function of tumor-associated sites before and 2–3 days after local OK-432 administration. Cells were isolated from tumor-associated exudate fluids, such as pleural effusions and ascites. The frequency of Treg cells before and after treatment with OK-432 was examined by staining with Abs for CD4, CD25, and Foxp3. The $Foxp3^+$ T-cell population in $CD4^+$ T cells was markedly reduced (Fig. 4A). Furthermore, the proportion of $Foxp3^+$ T cells in $CD4^+CD25^+$ T cells was also significantly reduced after OK-432 administration (Fig. 4A and B), indicating that the balance of helper T cells to Treg cells had changed.

We next addressed the suppressive activity of $CD4^+CD25^{high}$ T cells in tumor-associated exudate fluids. $CD4^+CD25^{high}$ T cells (highest 3% gate of $CD4^+CD25^+$ cells defined with peripheral blood was applied) were isolated from tumor-associated exudate fluids and cultured with $CD4^+CD25^-$ T cells from PBMCs with irradiated autologous APCs and anti-CD3 Ab. After OK-432 administration, as the volume of tumor-associated exudate fluids decreased, sufficient amounts of $CD4^+CD25^{high}$ T cells for proliferation assays were available only from two patients. $CD4^+CD25^-$ T-cell proliferation was analyzed as described in the *Materials and Methods*. There was a trend, albeit not significant, toward a decrease in Treg-cell function after OK-432 administration (Fig. 4C). In contrast, we did not observe any differences in frequency and function of Treg cells in PBMCs

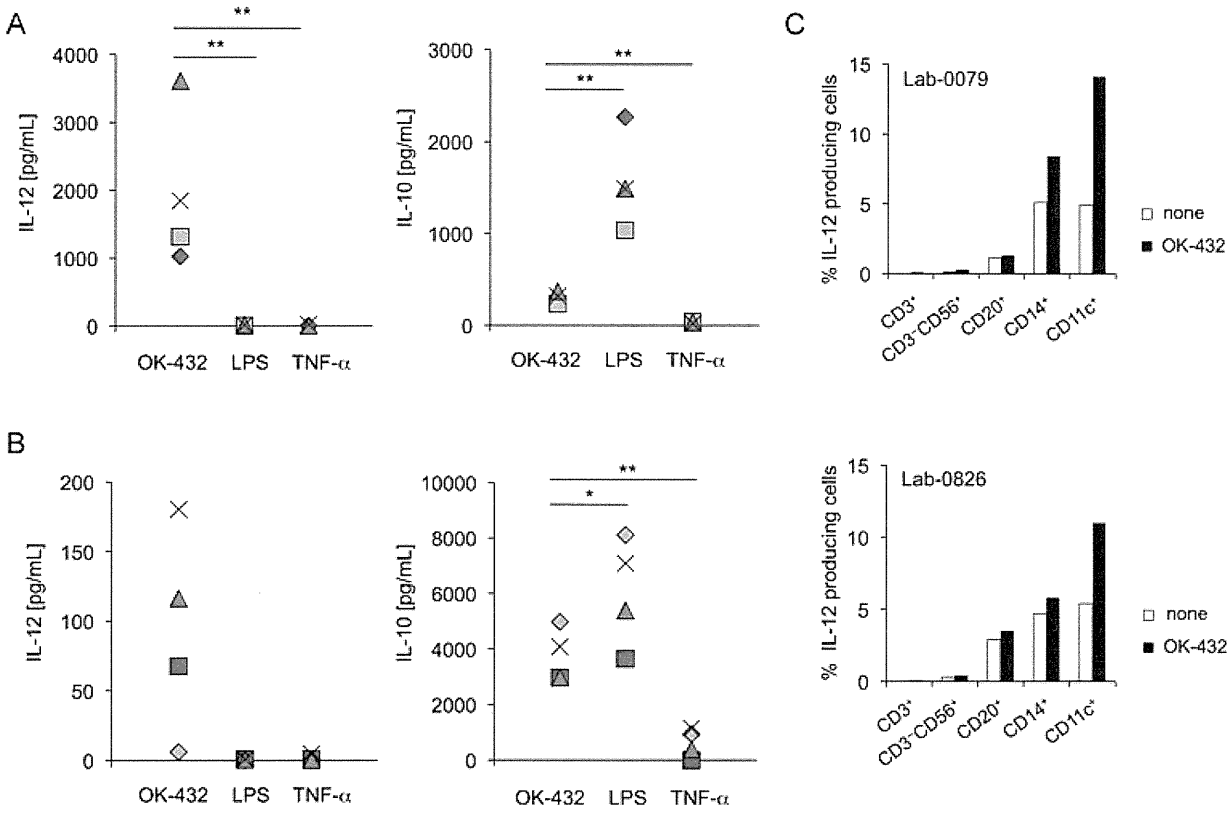

Figure 3. APCs stimulated with OK-432 produce significantly higher amounts of IL-12. (A) 1×10^5 CD3-depleted PBMCs from four healthy individuals were cultured with TNF-α (100 ng/mL), LPS (1 mg/mL), or OK-432 (1 μg/mL) and supernatant was collected 48 h later. IL-12p70 and IL-10 production was analyzed with ELISA. (B) 1×10^5 CD3-depleted PBMCs from four esophageal cancer patients were cultured as in (A) and supernatant was collected 48 h later. IL-12p70 and IL-10 production was analyzed with ELISA. (A, B) Each symbol represents an individual donor; data shown are from one experiment representative of at least two performed. (C) PBMCs from two healthy individuals were cultured with/without OK-432. Cells were subjected to staining with the indicated surface markers and then intracellular IL-12, and were analyzed by flow cytometry. Data of two donors from one experiment representative of at least two performed. $^*p < 0.05$ and $^{**}p < 0.01$ as compared with control, Student's *t*-test.

before and after OK-432 administration (data not shown). These data propose that in vivo injection of OK-432 decreases the local Treg-cell accumulation and function.

Origin of the repertoire of CD4$^+$ T-cell effectors elicited by vaccination with NY-ESO-1 and OK-432

To further explore the effect of OK-432 on the inhibition of in vivo Treg-cell activity, we also examined the potential of OK-432 as an adjuvant in a cancer vaccine. We have reported that high-avidity NY-ESO-1–specific CD4$^+$ T-cell precursors are present in naive CD45RA$^+$ populations and that their activation is rigorously suppressed by CD4$^+$CD25$^+$ Treg cells [20, 21]. We also found that synthetic peptide vaccination with incomplete Freund's adjuvant induces only peptide-specific CD4$^+$ T cells with low-avidity TCRs (recognition of >1 μM peptide but not naturally processed NY-ESO-1 protein), but not high-avidity CD4$^+$ T cells (recognition of naturally processed NY-ESO-1 protein or <0.1 μM peptide) that are susceptible to Treg-cell suppression [21]. Together, these data highlight the importance of blocking Treg-cell activity to allow activation/expansion of high-avidity NY-ESO-1–specific CD4$^+$ T-cell precursors. For this reason, we investigated whether high-avidity NY-ESO-1–specific CD4$^+$ T-cell precursors were activated by NY-ESO-1 protein vaccination with OK-432 as an adjuvant and were present in memory CD45RO$^+$ populations.

Samples from two patients who received vaccination with cholesteryl hydrophobized pullulan (CHP)-HER2 and NY-ESO-1 with OK-432 (Supporting Information Fig. 1) were available for this analysis. Whole CD4$^+$ T cells or CD4$^+$CD25$^-$CD45RO$^+$ (effector/memory) T cells before and after vaccination were presensitized with NY-ESO-1–overlapping peptides covering the entire sequence of NY-ESO-1 and specific CD4$^+$ T-cell induction was analyzed with ELISPOT assays. As the sample size was not sufficient to analyze specific CD4$^+$ T-cell induction within CD4$^+$CD25$^-$CD45RA$^+$ (naive) T cells, we analyzed whether NY-ESO-1–specific high-avidity CD4$^+$ T cells were induced from the CD4$^+$CD25$^-$CD45RO$^+$ (effector/memory) T-cell population after vaccination in Pt #1 (HLA-DR 4, 12 and HLA -DQ 4, 8) and #2 (HLA-DR 9, 15 and HLA-DQ 6, 9). Pt #1 exhibited spontaneously induced CD4$^+$ T-cell responses against NY-ESO-1_{91-110} before vaccination and the responses were maintained after extensive vaccination (Fig. 5A). These spontaneously

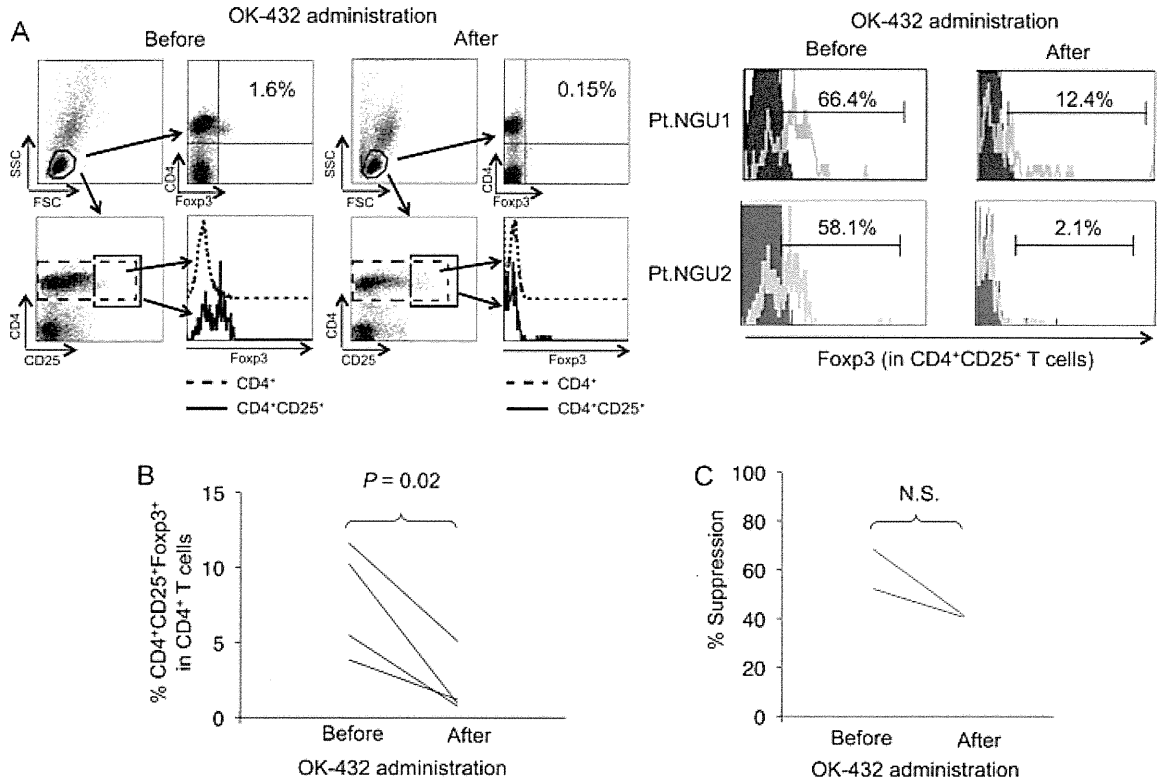

Figure 4. OK-432 administration into tumor-associated exudate fluids elicits reduction of local Treg-cell accumulation and function. Cells were isolated from tumor-associated exudate fluids (two pleural effusions or two ascites) and peripheral blood before and 2 days after OK-432 administration. (A) Cells were stained with anti-CD4, anti-CD25, and anti-Foxp3 Abs and were analyzed with flow cytometry. The staining pattern and gating method of a representative patient is shown (left); solid line histogram, Foxp3 expression in $CD4^+$ $CD25^+$ T cells; dotted line histogram, Foxp3 expression in $CD4^+$ T cells. Foxp3 expression in $CD4^+CD25^+$ T cells of two representative patients is shown (right); filled histogram, control staining; gray line histogram, Foxp3. (B) The percentage of $CD4^+CD25^+Foxp3^+$ cells in $CD4^+$ T cells is shown for $n = 4$ patients' samples. Statistical significance determined by Student's *t*-test. (C) 1×10^5 $CD4^+CD25^-$ T cells were isolated from PBMCs before OK-432 administration and cultured with irradiated autologous CD4-depleted PBMCs and anti-CD3 Ab in the presence or absence of 1×10^5 $CD4^+CD25^{high}$ T cells isolated from tumor-associated exudate fluids before and after OK-432 administration ($n = 2$). Data shown are from one experiment representative of two independent experiments.

induced NY-ESO-1_{91-110}–specific $CD4^+$ T cells were detected in the $CD4^+CD25^-CD45RO^+$ (effector/memory) T-cell population before and after vaccination. Following vaccination with NY-ESO-1 protein in the presence of OK-432, $CD4^+$ T-cell immune responses against NY-ESO-$1_{111-130}$ were newly elicited (Fig. 5A). These vaccine-induced NY-ESO-$1_{111-130}$–specific $CD4^+$ T cells were detected in the $CD4^+CD25^-CD45RO^+$ (effector/memory) T-cell population only after vaccination (Fig. 5A). In Pt #2, while specific $CD4^+$ T cells were not observed before vaccination, NY-ESO-$1_{119-141}$–specific $CD4^+$ T cells were elicited after vaccination. The vaccine-induced NY-ESO-$1_{119-141}$–specific $CD4^+$ T cells were also detected in the $CD4^+CD25^-CD45RO^+$ (effector/memory) T-cell population, as observed in Pt #1 (Fig. 5B).

NY-ESO-1 vaccination with OK-432 activates high-avidity preexisting NY-ESO-1–specific $CD4^+$ T-cells

We then asked whether vaccine-induced T cells had a high-affinity TCR that recognized naturally processed antigens [21, 28]. We established NY-ESO-1–specific $CD4^+$ T-cell clones. Four clones and a single clone that recognized different epitopes were generated from Pt #1 and Pt #2, respectively. Four minimal epitopes (NY-ESO-$1_{83-96,\ 94-109,\ 119-130,121-134}$) were defined from $CD4^+$ T-cell clones derived from Pt #1 (Fig. 6A and data not shown). Both spontaneously induced (#2–11) and vaccine-induced (#3–1) $CD4^+$ T-cell clones recognized naturally processed NY-ESO-1 protein and as little as 0.1 nM of peptide (Fig. 6A). One minimal epitope defined from Pt #2 was NY-ESO-$1_{122-133}$ and the vaccine-induced $CD4^+$ T-cell clone (#1–1) again recognized both the naturally processed NY-ESO-1 protein and as little as 0.1 nM of peptide (Fig. 6B), indicating that these T-cell clones had high-affinity TCRs against NY-ESO-1. Together, OK-432 as an adjuvant could overcome Treg-cell suppression and activate high-affinity preexisting NY-ESO-1–specific $CD4^+$ T-cell precursors.

Discussion

While a subset of patients treated with immunotherapy has been shown to experience objective and durable clinical responses, it is becoming increasingly clear that several mechanisms

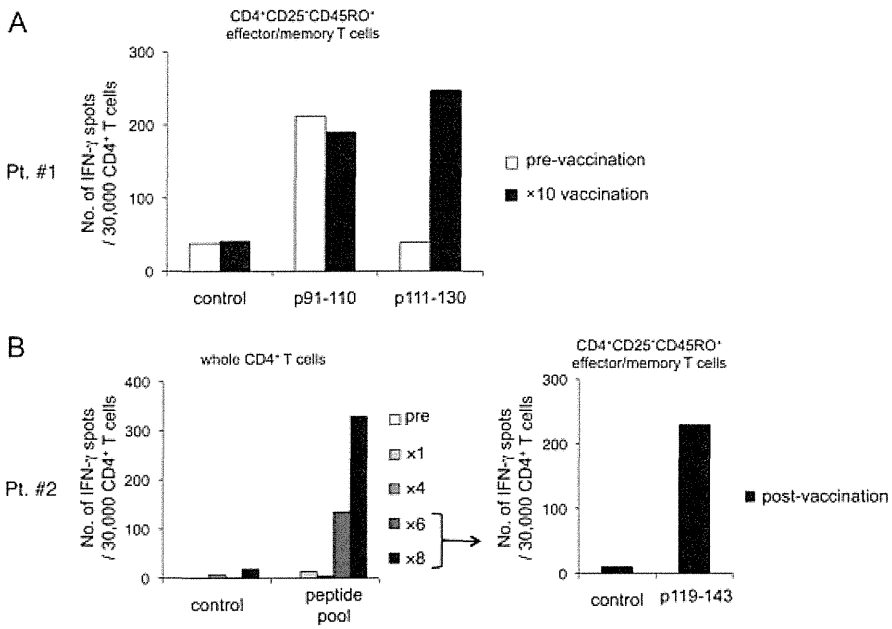

Figure 5. Vaccination with OK-432 elicits NY-ESO-1–specific effector/memory $CD4^+$ T cells $CD4^+CD25^-CD45RO^+$ T cells or unfractionated $CD4^+$ T cells were prepared from PBMCs of (A) Pt #1 (HLA-DR 4, 12 -DQ 4, 8) and (B) Pt #2 (HLA-DR 9, 15 -DQ 6, 9) before and after vaccination as described in the *Materials and Methods*; 3–5 × 10^5 $CD4^+CD25^-CD45RO^+$ T cells or unfractionated $CD4^+$ T cells were cultured with 3–5 × 10^5 CD4-depleted PBMCs pulsed with 10 μM pooled peptides covering the entire sequence of NY-ESO-1 for 3 weeks. Induction of NY-ESO-1–specific IFN-γ production was analyzed by ELISPOT. Data shown are from one experiment representative of at least two experiments performed.

downregulate antitumor immunity during the course of the immune response and play a major role in limiting the effectiveness of cancer immunity [6, 35, 36]. A plethora of cell types, cell surface molecules, and soluble factors mediate this suppressive activity [3, 6, 35, 36]. Among them, $CD4^+CD25^+Foxp3^+$ Treg cells play a crucial role by suppressing a wide variety of immune responses, and finding ways to control Treg-cell suppression is a major priority in this field [6, 7]. In this study, we showed the potential of OK-432 (a penicillin-inactivated and lyophilized preparation of *Streptococcus pyrogenes*) which stimulates TLR signals [30, 33, 34] to control Treg-cell suppression, supporting the idea that OK-432 may be a promising adjuvant for cancer vaccines by inhibiting Treg-cell suppression and by augmenting induction of tumor-specific T cells against coadministered protein antigens.

Appropriate adjuvant combinations, such as those that are MyD88-dependent or MyD88-independent, or those that are TRIF-coupled and include endosomal signals, are known to synergistically activate DCs with regard to the production of inflammatory cytokines [37, 38]. As OK-432 is derived from bacterial components, its capacity to bind a combination of various TLRs makes it attractive. It has been shown that OK-432 exhibits antitumor effects through TLR-2, TLR-4, and TLR-9 using knockout mice for each TLR [30, 33, 34]. Alternatively, OK-432 reportedly stimulates DCs through the β_2-integrin system rather than via TLR signals [29]. In the presence of OK-432, Treg cells slightly proliferated with TCR stimulation. TLR2 triggering results in a temporary loss of the anergic status of Treg cells and is associated with loss of Treg-cell suppressive function [24, 25]. The perturbation of Treg-cell anergy by OK-432 through TLR2 stimulation may play a role, at least in part, in the inhibition of Treg-cell suppressive function.

In accordance with previous reports [29, 34], we showed that APCs, including $CD11c^+$ and $CD14^+$ cells (monocytes, macrophage, and DCs), stimulated with OK-432 exhibited significantly higher production of IL-12 as compared with that of LPS- or TNF-α–matured APCs, and that OK-432–induced IL-12 from these APCs was a critical component for abrogating Treg-cell activity. Additionally, we found that monocyte-derived DCs stimulated with OK-432 produced significantly higher amounts of IL-12 compared with DCs stimulated with LPS or TNF-α (Supporting Information Fig. 2). It has been reported that IL-12 receptor expressed on effector T cells, but not on Treg cells has a critical role for abrogating Treg-cell suppression by IL-12 in mice [39, 40]. In accordance with this, downregulation of IL-12 receptors by siRNA on effector cells partially abrogated the OK-432–induced inhibition of Treg-cell suppressive activity (Supporting Information Fig. 3). IL-12 receptor was induced in both effector T cells and Treg cells after activation (Supporting Information Fig. 3). We attempted to downregulate the IL-12 receptor on Treg cells with siRNA to explore the exact target(s) of IL-12, however, the limitation in the availability of human materials hampered these analyses. Thus, IL-12 produced by APCs on the OK-432 stimulation could have two (or more) mutually compatible activities, (i) rendering effector cells resistant to Treg-cell suppression and (ii) inhibiting Treg-cell suppressive function directly, though the in vivo data argue against direct inhibition of Treg-cell suppression [39, 40].

Local administration of OK-432 reduced the number of $CD4^+CD25^+Foxp3^+$ Treg cells in tumor-associated exudate fluids. After administration of OK-432, local chemokine gradient may be changed and infiltration of Treg cells may be blocked [6, 13]. Alternatively, the inflammatory environment after OK-432 administration may be suitable for effector T-cell activation and IL-2, that is critical for Treg-cell survival and function [41], may not be adequately provided, as observed during severe *Toxoplasma gondii* infection [42]. In addition, suppressive function of $CD4^+CD25^{high}$ T cells in tumor-associated

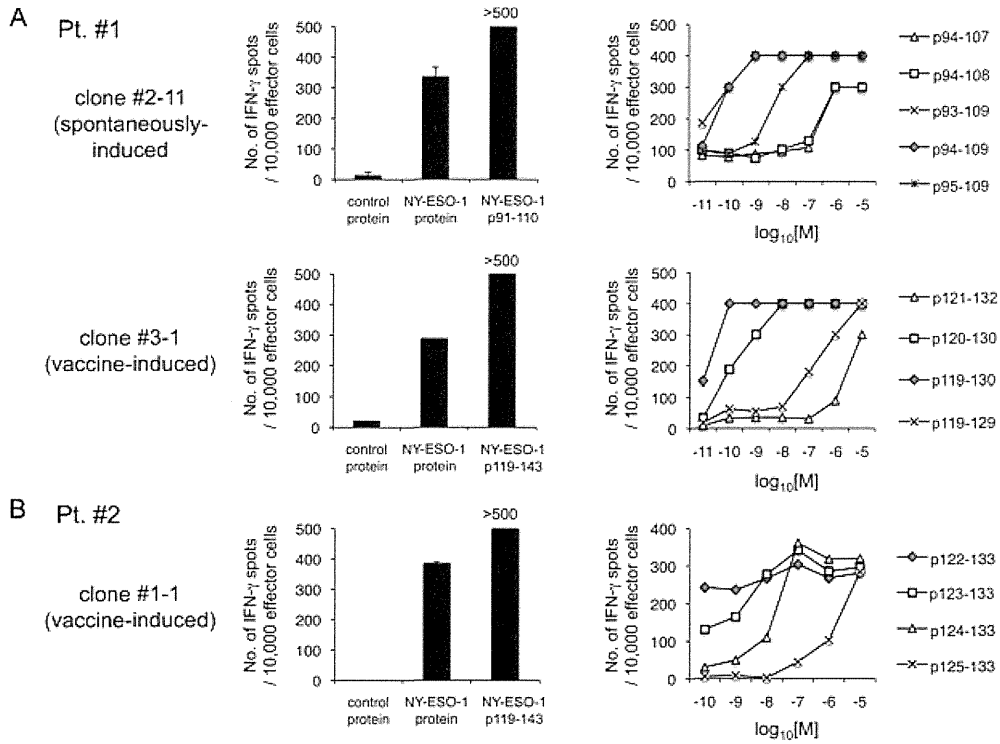

Figure 6. Vaccination with OK-432 activates high-avidity NY-ESO-1–specific CD4$^+$ T cells. NY-ESO-1–specific CD4$^+$ T-cell clones were generated from PBMCs of patients harboring NY-ESO-1–specific CD4$^+$ T cells. CD4$^+$ T-cell clones from (A) Pt. #1 and (B) Pt. #2 were stimulated and expanded by 30 ng/mL anti-CD3 Ab in the presence of 20 U/mL IL-2 and irradiated PBMCs and EBV-transformed human B lymphocytes as feeder cells. A couple of weeks later, these NY-ESO-1–specific CD4$^+$ T cell clones (1×10^4/well) were cultured with 1×10^4 NY-ESO-1 protein-pulsed DCs or 2×10^4 EBV-B cells pulsed with graded amounts of peptides and NY-ESO-1–specific IFN-γ production was analyzed by ELISPOT. Data are shown as mean ± SD of two replicates and are from one experiments representative of at least two experiments performed.

exudate fluids was reduced after OK-432 treatment in accordance with decreased expression of Foxp3 [43]. Considering the fact that IL-12, a main effector molecule induced by OK-432, renders effector cells resistant to Treg-cell suppression, direct administration of OK-432 may change the immunological balance in the local microenvironment from suppression by Treg cells to activation of helper T cells by augmenting helper T-cell activity. However, the sample size of patients analyzed in this study was relatively small and warrants cautious interpretation.

We have previously shown that while naive NY-ESO-1–specific CD4$^+$ T-cell precursors are present in wide range of healthy individuals and cancer patients, their activation is kept under stringent CD4$^+$CD25$^+$ Treg-cell control [20, 21, 28]. Using OK-432 as an adjuvant, we detected high-affinity NY-ESO-1–specific CD4$^+$ T cells in effector/memory population after vaccination in two esophageal cancer patients. In Pt #1, we found two responses; spontaneous and vaccine-induced NY-ESO-1–specific CD4$^+$ T cells. Both of them exhibited a similar efficiency to recognize titrated peptide, indicating that these NY-ESO-1–specific CD4$^+$ T cells had TCRs with similar affinity and were likely activated from naive high-affinity NY-ESO-1–specific CD4$^+$ T-cell precursors. Vaccination with minimal peptide in incomplete Freund's adjuvant fails to activate high-affinity NY-ESO-1–specific CD4$^+$ T-cell precursors, rather it dominantly expands low-avidity effector/memory CD4$^+$ T cells that cannot recognize naturally processed antigens [21]. In addition, following DNA vaccination covering the entire sequence of NY-ESO-1, high-avidity NY-ESO-1–specific CD4$^+$ T cells were not detected persistently because of rapid suppression by Treg cells [44]. While these data suggest a critical role for the inhibition of Treg-cell suppression by OK-432 in the activation of high-affinity NY-ESO-1–specific CD4$^+$ T-cell precursors, it is still difficult to obtain conclusive evidence without direct in vivo Treg-cell inhibition/depletion. To formally address this issue, clinical trials using Treg-cell depletion reagents and another clinical trial having two arms of patients receiving NY-ESO-1 with/without OK-432 would be required.

Certain types of immunization methods or DC stimulations elicit/augment CD4$^+$CD25$^+$ Treg cells in vivo [10–12, 45]. As many tumor-associated antigens recognized by autologous tumor-reactive lymphocytes are antigenically normal self-constituents [1–3], they also could be recognized with CD4$^+$CD25$^+$ Treg cells. Given that a proportion of cancer/testis antigens are targets of Treg cells [46], it is necessary to avoid unwanted activation of cancer/testis antigen-specific CD4$^+$CD25$^+$ Treg cells. Though the sample size of patients analyzed in this study was small and warrants cautious interpretation, including OK-432 in vaccine components as an adjuvant would be a promising strategy to establish favorable circumstances for stimulating effector T cells by inhibiting Treg-cell activation. Furthermore, since this agent has a long history and is widely applied as an anticancer drug, particularly

in Japan, its clinical safety profile has been already established. Our data provide a critical cue for effective cancer vaccines and immunotherapy during antigen priming through modulation of $CD4^+CD25^+$ Treg-cell function.

Materials and methods

Blood samples

All healthy donors were subjects with no history of autoimmune disease. PBMCs, pleural effusions, or ascites from cancer patients were collected before and after local administration of OK-432 based on the protocol approved by the Human Ethics Committees of Mie University Graduate School of Medicine and Nagasaki University Graduate School of Medicine. PBMCs from esophageal cancer patients enrolled in a clinical trial of CHP-NY-ESO-1 and CHP-HER2 vaccination with OK-432 [47] (Supporting Information Fig. 1) were collected based on the protocol approved by the Human Ethics Committees of Mie University Graduate School of Medicine and Kitano Hospital. The clinical trial was conducted in full conformity with the current version of the Declaration of Helsinki and was registered as NCT00291473 of Clinical Trial.gov, and 000001081 of UMIN Clinical Trial Registry. All samples were collected after written informed consent.

Abs and reagents

Synthetic peptides of NY-ESO-1_{1-20} (MQAEGRGTGGSTGDADGPGG), NY-ESO-1_{11-30} (STGDADGPGGPGIPDGPGGN), NY-ESO-1_{21-40} (PGIPDGPGGNAGGPGEAGAT), NY-ESO-1_{31-50} (AGGPGEAGATGGRGPRGAGA), NY-ESO-1_{41-60} (GGRGPRGAGAARASGPGGGA), NY-ESO-1_{51-70} (ARASGPGGGAPRGPHGGAAS), NY-ESO-1_{61-80} (PRGPHGGAASGLNGCCRCGA), NY-ESO-1_{71-90} (GLNGCCRCGARGPESRLLEF), NY-ESO-1_{81-100} (RGPESRLLEFYLAMPFATPM), NY-ESO-1_{91-110} (YLAMPFATPMEAELARRSLA), NY-ESO-$1_{101-120}$ (EAELARRSLAQDAPPLPVPG), NY-ESO-$1_{111-130}$ (QDAPPLPVPGVLLKEFTVSG), NY-ESO-$1_{119-143}$ (PGVLLKEFTVSGNILTIRLTAADHR), NY-ESO-$1_{131-150}$ (NILTIRLTAADHRQLQLSIS), NY-ESO-$1_{139-160}$ (AADHRQLQLSISSCLQQLSLLM), NY-ESO-$1_{151-170}$ (SCLQQLSLLMWITQCFLPVF), NY-ESO-$1_{161-180}$ (WITQCFLPVFLAQPPSGQRR), and HIV $P17_{37-51}$ (ASRELERFAVNPGLL) [48] were obtained from Invitrogen (Carlsbad, CA, USA). Recombinant NY-ESO-1 protein was prepared using similar procedures as described previously [49]. OK-432 was purchased from Chugai Pharmaceutical (Tokyo, Japan). LPS (*Escherichia coli* 055:B5) was obtained from Sigma (St. Louis, MO, USA). Purified and FITC-conjugated anti-IL-12 (C8.6; mouse IgG1), purified anti-IL-6 (MQ2–13A5; rat IgG1), purified anti-IFN-γ (NIB42; mouse IgG1), purified anti-IL-23 (HNU2319; mouse IgG1), PE-conjugated anti-CD20 (2H7; mouse IgG2b) and PE-conjugated anti-CD56 (MEM188; mouse IgG2a) Abs were purchased from eBioscience (San Diego, CA, USA). Purified anti-IL-1β Ab (8516; mouse IgG1) was purchased from R&D Systems (Minneapolis, MN, USA). PE-conjugated anti-CD14 (MφP9; mouse IgG2b), PE-conjugated anti-CD45RA (HI100; mouse IgG2b), PerCP-conjugated anti-CD4 (RPA-T4; mouse IgG1), and FITC-conjugated anti-CD4 (RPA-T4; mouse IgG1), Foxp3 (259D; mouse IgG1), and CD45RO (UCHL1; mouse IgG2a) Abs were purchased from BD Biosciences (Franklin Lakes, NJ, USA). PerCP-Cy5.5-conjugated anti-CD11c Ab (3.9; mouse IgG1) was obtained from Biolegend (San Diego CA, USA). PE-conjugated anti-CD25 Ab (4E3; mouse IgG2b) was obtained from Miltenyi Biotec (Bergisch Gladbach, Germany). Recombinant IL-6, IL-12, and TNF-α were purchased from PeproTech (Rocky Hill, NJ, USA).

Intracellular cytokine staining

PBMCs were cultured with/without OK-432 and GolgiStop reagent (BD Biosciences) for 20 h. Cells were stained for cell surface markers and then for intracellular cytokine (IL-12) after permeabilization. Results were analyzed by flow cytometry (FACSCanto; BD Biosciences).

Generation of NY-ESO-1–specific $CD4^+$ T cells

NY-ESO-1–specific $CD4^+$ T cells were elicited as described previously [20]. Briefly, $CD4^+$ T cells and $CD4^+CD25^-$ T cells were isolated from PBMCs using a $CD4^+CD25^+$ Treg Isolation Kit (Miltenyi Biotec). $CD4^+CD25^-$ T cells were further separated into $CD45RO^+$ T cells or $CD45RA^+$ T cells by FACSAria (BD Bioscience) after staining with anti-CD45RO and CD45RA Abs. $CD4^-$ PBMCs pulsed with 10 μM of peptide overnight were used as APCs. After irradiation, 5×10^5 APCs were added to round-bottom 96-well plates (Nunc, Roskilde, Denmark) containing $1–5 \times 10^5$ unfractionated $CD4^+$ or $CD4^+CD25^-CD45RO^+$ T cells and were fed with 10 U/mL IL-2 (Kindly provided by Takeda Pharmaceutical, Osaka, Japan) and 20 ng/mL IL-7 (R&D Systems). Subsequently, one-half of medium was replaced by fresh medium containing IL-2 (20 U/ml) and IL-7 (40 ng/mL) twice per week.

Generation of NY-ESO-1–specific $CD4^+$ T-cell clones

Cloning was performed by limited dilution as described previously [50]. Briefly, NY-ESO-1–specific $CD4^+$ T cell lines (0.3 cells/well) were stimulated and expanded in the presence of irradiated 5×10^4 cells/well PBMCs and 1×10^4 cells/well irradiated EBV-transformed human B lymphocytes with 10% AB serum, 20 U/ml IL-2, and 30 ng/mL anti-CD3 Ab (OKT3; eBioscience) in 96-well round-bottom plates.

Proliferation assay

$CD4^+CD25^-$ T cells were cultured with 1×10^5 irradiated CD4-depleted PBMCs and stimulated with 0.5 μg/mL anti-CD3 Ab

(OKT3, eBioscience) in round-bottom 96-well plates. $CD4^+CD25^{high}$ Treg cells (highest 3% of $CD4^+CD25^+$ cells) were purified with FACSAria (BD Biosciences), and graded numbers of them added in the culture as indicated in figure legends. Proliferation was evaluated by ^{3}H-thymidine with 1 μCi/well for the last 18 h of 6-day culture. ^{3}H-thymidine incorporation was measured by a scintillation counter.

ELISPOT (enzyme-linked immunospot) assay

The number of IFN-γ secreting antigen-specific $CD4^+$ T cells was assessed by ELISPOT assays as described [20, 21]. Briefly, flat-bottomed, 96-well nitrocellulose-coated microtiter plates (Millipore, Bedford, MA, USA) were coated with anti-IFN-γ Ab (1-D1K; MABTECH, Stockholm, Sweden). The presensitized T cells and phytohaemagglutinin (PHA HA15; Murex Diagnostics, Dartford, UK) activated $CD4^+$ T cells, EBV-transformed human B lymphocytes or DCs pulsed with 10 μM of peptides or 25 μg/mL protein overnight were added to each well and incubated for 24 h. Spots were developed using biotinylated anti-IFN-γ Ab (7-B6–1-biotin; MABTECH), alkaline phosphatase conjugated streptavidin (Roche, Mannheim, Germany) and 5-bromo-4-chloro-3-indolyl phosphate/nitroblue tetrazolium (Sigma) and counted with C.T.L. Immunospot analyzer and software (Cellular Technologies, Cleveland, OH, USA).

Preparation of monocyte-derived DCs

Monocyte-derived DCs were generated from PBMCs as previously described with some modifications [51]. Briefly, $CD14^+$ monocytes were enriched by positive selection using CD14 Microbeads (Miltenyi Biotec). Monocytes were cultured in the presence of 20 ng/mL GM-CSF (Immunex, Seattle, WA, USA) and 20 ng/mL IL-4 (R&D systems) in RPMI1640 supplemented with 2.5% fetal calf serum. Medium was replaced by fresh medium containing cytokines 3 days later. On day 6, cells were harvested and used for subsequent experiments.

ELISA

The concentration of IL-12p70 and IL-10 was measured by ELISA Kit (eBioscicence) according to the instruction provided by the manufacturer.

Statistical analysis

Statistical significance was evaluated by Student's *t*-test; *p* values less than 0.05 are considered significant.

Acknowledgments: This article is dedicated to the memory of Lloyd J. Old, M.D. We thank Drs. T. Takahashi and J. B. Wing for critical reading of the manuscript, and L. Wang, C. Brooks, E. Krapavinsky, E. Ritter, and D. Santiago for technical support.
This study was supported by Grant-in-Aid for Scientific Research on Priority Areas (No. 17016031, H. Shiku, and No. 20015019, H. Nishikawa) and Grants-in-Aid for Scientific Research (B) (No. 23300354, H. Nishikawa), the Cancer Research Institute Investigator Award (H. Nishikawa) and Cancer Vaccine Collaborative Grant for Immunological Monitoring (S. Gnjatic, G. Ritter and L.J. Old), Cancer Research Grant from Foundation of Cancer Research Promotion (H. Nishikawa), Takeda Science Foundation (H. Nishikawa), Kato Memorial Bioscience Foundation (H. Nishikawa), the Sagawa Foundation for Promotion of Cancer Research (H. Nishikawa), and Senri Life Science Foundation (H. Nishikawa). MH is a research fellow of the Japan Society for the Promotion of Science.

Conflicts of interest: The authors declare no financial or commercial conflict of interest.

References

1 **Kawakami, Y. and Rosenberg, S. A.**, Human tumor antigens recognized by T-cells. *Immunol. Res.* 1997. **16**: 313–339.

2 **Scanlan, M. J., Gure, A. O., Jungbluth, A. A., Old, L. J. and Chen, Y. -T.**, Cancer/testis antigens: an expanding family of targets for cancer immunotherapy. *Immunol. Rev.* 2002. **188**: 22–32.

3 **Boon, T., Coulie, P. G., Van den Eynde, B. J. and van der Bruggen, P.**, Human T cell responses against melanoma. *Annu. Rev. Immunol.* 2006. **24**: 175–208.

4 **Shevach, E. M.**, $CD4^+$ $CD25^+$ suppressor T cells: more questions than answers. *Nat. Rev. Immunol.* 2002. **2**: 389–400.

5 **Sakaguchi, S.**, Naturally arising $CD4^+$ regulatory T cells for immunologic self-tolerance and negative control of immune responses. *Annu. Rev. Immunol.* 2004. **22**: 531–562.

6 **Nishikawa, H. and Sakaguchi, S.**, Regulatory T cells in tumor immunity. *Int. J. Cancer* 2010. **127**: 759–767.

7 **Sakaguchi, S., Miyara, M., Costantino, C. M. and Hafler, D. A.**, $FOXP3^+$ regulatory T cells in the human immune system. *Nat. Rev. Immunol.* 2010. **10**: 490–500.

8 **Onizuka, S., Tawara, I., Shimizu, J., Sakaguchi, S., Fujita, T. and Nakayama, E.**, Tumor rejection by in vivo administration of anti-CD25 (interleukin-2 receptor α) monoclonal antibody. *Cancer Res.* 1999. **59**: 3128–3133.

9 **Shimizu, J., Yamazaki, S. and Sakaguchi, S.**, Induction of tumor immunity by removing $CD25^+CD4^+$ T cells: a common basis between tumor immunity and autoimmunity. *J. Immunol.* 1999. **163**: 5211–5218.

10 **Nishikawa, H., Kato, T., Tanida, K., Hiasa, A., Tawara, I., Ikeda, H., Ikarashi, Y. et al.**, $CD4^+$ $CD25^+$ T cells responding to serologically defined

autoantigens suppress antitumor immune responses. *Proc. Natl. Acad. Sci. USA.* 2003. **100**: 10902–10906.

11 **Nishikawa, H., Kato, T., Tawara, I., Saito, K., Ikeda, H., Kuribayashi, K., Allen, P. M. et al.**, Definition of target antigens for naturally occurring $CD4^+$ $CD25^+$ regulatory T cells. *J. Exp. Med.* 2005. **201**: 681–686.

12 **Nishikawa, H., Kato, T., Tawara, I., Takemitsu, T., Saito, K., Wang, L., Ikarashi, Y. et al.**, Accelerated chemically induced tumor development mediated by $CD4^+CD25^+$ regulatory T cells in wild-type hosts. *Proc. Natl. Acad. Sci. USA.* 2005. **102**: 9253–9257.

13 **Curiel, T. J., Coukos, G., Zou, L., Alvarez, X., Cheng, P., Mottram, P., Evdemon-Hogan, M. et al.**, Specific recruitment of regulatory T cells in ovarian carcinoma fosters immune privilege and predicts reduced survival. *Nat. Med.* 2004. **10**: 942–949.

14 **Sato, E., Olson, S. H., Ahn, J., Bundy, B., Nishikawa, H., Qian, F., Jungbluth, A. A. et al.**, Intraepithelial $CD8^+$ tumor-infiltrating lymphocytes and a high $CD8^+$/regulatory T cell ratio are associated with favorable prognosis in ovarian cancer. *Proc. Natl. Acad. Sci. USA.* 2005. **102**: 18538–18543.

15 **Dannull, J., Su, Z., Rizzieri, D., Yang, B. K., Coleman, D., Yancey, D., Zhang, A. et al.**, Enhancement of vaccine-mediated antitumor immunity in cancer patients after depletion of regulatory T cells. *J. Clin. Invest.* 2005. **115**: 3623–3633.

16 **Chen, Y.-T., Scanlan, M. J., Sahin, U., Tureci, O., Gure, A. O., Tsang, S., Williamson, B. et al.**, A testicular antigen aberrantly expressed in human cancers detected by autologous antibody screening. *Proc. Natl. Acad. Sci. U S A.* 1997. **94**: 1914–1918.

17 **Gnjatic, S., Nishikawa, H., Jungbluth, A. A., Gure, A. O., Ritter, G., Jager, E., Knuth, A. et al.**, NY-ESO-1: review of an immunogenic tumor antigen. *Adv. Cancer Res.* 2006. **95**: 1–30.

18 **Gnjatic, S., Nagata, Y., Jager, E., Stockert, E., Shankara, S., Roberts, B. L., Mazzara, G. P. et al.**, Strategy for monitoring T cell responses to NY-ESO-1 in patients with any HLA class I allele. *Proc. Natl. Acad. Sci. U S A.* 2000. **97**: 10917–10922.

19 **Danke, N. A., Koelle, D. M., Yee, C., Beheray, S. and Kwok, W. W.**, Autoreactive T cells in healthy individuals. *J. Immunol.* 2004. **172**: 5967–5972.

20 **Nishikawa, H., Jager, E., Ritter, G., Old, L. J. and Gnjatic, S.**, $CD4^+CD25^+$ regulatory T cells control the induction of antigen-specific $CD4^+$ helper T cell responses in cancer patients. *Blood* 2005. **106**: 1008–1011.

21 **Nishikawa, H., Qian, F., Tsuji, T., Ritter, G., Old, L. J., Gnjatic, S. and Odunsi, K.**, Influence of $CD4^+CD25^+$ regulatory T cells on low/high-avidity $CD4^+$ T cells following peptide vaccination. *J. Immunol.* 2006. **176**: 6340–6346.

22 **Iwasaki, A. and Medzhitov, R.**, Toll-like receptor control of the adaptive immune responses. *Nat. Immunol.* 2004. **5**: 987–995.

23 **Pasare, C. and Medzhitov, R.**, Toll pathway-dependent blockade of $CD4^+CD25^+$ T cell-mediated suppression by dendritic cells. *Science* 2003. **299**: 1033–1036.

24 **Sutmuller, R. P., den Brok, M. H., Kramer, M., Bennink, E. J., Toonen, L. W., Kullberg, B. J., Joosten, L. A. et al.**, Toll-like receptor 2 controls expansion and function of regulatory T cells. *J. Clin. Invest.* 2006. **116**: 485–494.

25 **Liu, H. Y., Komai-Koma, M., Xu, D. and Liew, F. Y.**, Toll-like receptor 2 signaling modulates the functions of $CD4^+CD25^+$ regulatory T cells. *Proc. Natl. Acad. Sci. USA.* 2006. **103**: 7048–7053.

26 **Yang, Y., Huang, C. T., Huang, X. and Pardoll, D. M.**, Persistent Toll-like receptor signals are required for reversal of regulatory T cell-mediated CD8 tolerance. *Nat. Immunol.* 2004. **5**: 508–515.

27 **Nishikawa, H., Sato, E., Briones, G., Chen, L. M., Matsuo, M., Nagata, Y., Ritter, G. et al.**, In vivo antigen delivery by a *Salmonella typhimurium* type III secretion system for therapeutic cancer vaccines. *J. Clin. Invest.* 2006. **116**: 1946–1954.

28 **Nishikawa, H., Tsuji, T., Jager, E., Briones, G., Ritter, G., Old, L. J., Galan, J. E. et al.**, Induction of regulatory T cell-resistant helper $CD4^+$ T cells by bacterial vector. *Blood* 2008. **111**: 1404–1412.

29 **Nakahara, S., Tsunoda, T., Baba, T., Asabe, S. and Tahara, H.**, Dendritic cells stimulated with a bacterial product, OK-432, efficiently induce cytotoxic T lymphocytes specific to tumor rejection peptide. *Cancer Res.* 2003. **63**: 4112–4118.

30 **Okamoto, M., Oshikawa, T., Tano, T., Ohe, G., Furuichi, S., Nishikawa, H., Ahmed, S. U. et al.**, Involvement of toll-like receptor 4 signaling in interferon-γ production and antitumor effect by streptococcal agent OK-432. *J. Natl. Cancer Inst.* 2003. **95**: 316–326.

31 **Okamoto, M., Oshikawa, T., Tano, T., Ahmed, S. U., Kan, S., Sasai, A., Akashi, S. et al.**, *Mechanism of anticancer host response* induced by OK-432, a streptococcal preparation, mediated by phagocytosis and Toll-like receptor 4 signaling. *J. Immunother.* 2006. **29**: 78–86.

32 **Ono, T., Harada, M., Yamada, A., Tanaka, M., Takao, Y., Tanaka, Y., Mine, T. et al.**, Antitumor effects of systemic and local immunization with a CTL-directed peptide in combination with a local injection of OK-432. *Clin. Cancer Res.* 2006. **12**: 1325–1332.

33 **Oshikawa, T., Okamoto, M., Tano, T., Sasai, A., Kan, S., Moriya, Y., Ryoma, Y. et al.**, Antitumor effect of OK-432-derived DNA: one of the active constituents of OK-432, a streptococcal immunotheropeutic agent. *J. Immunother.* 2006. **29**: 143–150.

34 **Okamoto, M., Furuichi, S., Nishioka, Y., Oshikawa, T., Tano, T., Ahmed, S. U., Takeda, K. et al.**, Expression of toll-like receptor 4 on dendritic cells is significant for anticancer effect of dendritic cell-based immunotherapy in combination with an active component of OK-432, a streptococcal preparation. *Cancer Res.* 2004. **64**: 5461–5470.

35 **Rosenberg, S. A., Yang, J. C. and Restifo, N. P.**, Cancer immunotherapy: moving beyond current vaccines. *Nat. Med.* 2004. **10**: 909–915.

36 **Dougan, M. and Dranoff, G.**, Immune therapy for cancer. *Annu. Rev. Immunol.* 2009. **27**: 83–117.

37 **Napolitani, G., Rinaldi, A., Bertoni, F., Sallusto, F. and Lanzavecchia, A.**, Selected Toll-like receptor agonist combinations synergistically trigger a T helper type 1-polarizing program in dendritic cells. *Nat. Immunol.* 2005. **6**: 769–776.

38 **Warger, T., Osterloh, P., Rechtsteiner, G., Fassbender, M., Heib, V., Schmid, B., Schmitt, E. et al.**, Synergistic activation of dendritic cells by combined toll-like receptor ligation induces superior CTL responses in vivo. *Blood* 2006. **108**: 544–550.

39 **King, I. L. and Segal, B. M.**, Cutting edge: IL-12 induces $CD4^+CD25^-$ T cell activation in the presence of T regulatory cells. *J. Immunol.* 2005. **175**: 641–645.

40 **Zhao, J. X., Zhao, J. C. and Perlman, S.**, Differential effects of IL-12 on Tregs and non-Treg T cells: roles of IFN-γ, IL-2 and IL-2R. *Plos One* 2012. **7**: e46241.

41 **Setoguchi, R., Hori, S., Takahashi, T. and Sakaguchi, S.**, Homeostatic maintenance of natural $Foxp3^+$ $CD25^+$ $CD4^+$ regulatory T cells by interleukin (IL)-2 and induction of autoimmune disease by IL-2 neutralization. *J. Exp. Med.* 2005. **201**: 723–735.

42 **Oldenhove, G., Bouladoux, N., Wohlfert, E. A., Hall, J. A., Chou, D., Dos Santos, L., O'Brien, S. et al.**, Decrease of $Foxp3^+$ Treg cell number and

acquisition of effector cell phenotype during lethal infection. *Immunity* 2009. **31**: 772–786.

43 **Wan, Y. S. Y. and Flavell, R. A.**, Regulatory T-cell functions are subverted and converted owing to attenuated Foxp3 expression. *Nature* 2007. **445**: 766–770.

44 **Gnjatic, S., Altorki, N. K., Tang, D. N., Tu, S. M., Kundra, V., Ritter, G., Old, L. J. et al.**, NY-ESO-1 DNA vaccine induces T-cell responses that are suppressed by regulatory T cells. *Clin. Cancer Res.* 2009. **15**: 2130–2139.

45 **Zhou, G., Drake, C. G. and Levitsky, H. I.**, Amplification of tumor-specific regulatory T cells following therapeutic cancer vaccines. *Blood* 2006. **107**: 628–636.

46 **Bonertz, A., Weitz, J., Pietsch, D. H. K., Rahbari, N. N., Schlude, C., Ge, Y. Z., Juenger, S. et al.**, Antigen-specific Tregs control T cell responses against a limited repertoire of tumor antigens in patients with colorectal carcinoma. *J. Clin. Invest.* 2009. **119**: 3311–3321.

47 **Aoki, M., Ueda, S., Nishikawa, H., Kitano, S., Hirayama, M., Ikeda, H., Toyoda, H. et al.**, Antibody responses against NY-ESO-1 and HER2 antigens in patients vaccinated with combinations of cholesteryl pullulan (CHP)-NY-ESO-1 and CHP-HER2 with OK-432. *Vaccine* 2009. **27**: 6854–6861.

48 **Gnjatic, S., Atanackovic, D., Jager, E., Matsuo, M., Selvakumar, A., Altorki, N. K., Maki, R. G. et al.**, Survey of naturally occurring $CD4^+$ T cell responses against NY-ESO-1 in cancer patients: correlation with antibody responses. *Proc. Natl. Acad. Sci. U S A.* 2003. **100**: 8862–8867.

49 **Stockert, E., Jager, E., Chen, Y.-T., Scanlan, M. J., Gout, I., Karbach, J., Arand, M. et al.**, A survey of the humoral immune response of cancer patients to a panel of human tumor antigens. *J. Exp. Med.* 1998. **187**: 1349–1354.

50 **Riddell, S. R. and Greenberg, P. D.**, The use of anti-CD3 and anti-CD28 monoclonal-antibodies to clone and expand human antigen-specific T-cells. *J. Immunol. Methods* 1990. **128**: 189–201.

51 **Nagata, Y., Ono, S., Matsuo, M., Gnjatic, S., Valmori, D., Ritter, G., Garrett, W. et al.**, Differential presentation of a soluble exogenous tumor antigen, NY-ESO-1, by distinct human dendritic cell populations. *Proc. Natl. Acad. Sci. U S A.* 2002. **99**: 10629–10634.

Abbreviation: **CHP**: cholesteryl hydrophobized pullulan

Full correspondence: Dr. Hiroyoshi Nishikawa, Experimental Immunology, Immunology Frontier Research Center, Osaka University, 3-1 Yamadaoka, Suita, Osaka 565-0871, Japan
Fax: +81-6-6879-4464
e-mail: nisihiro@ifrec.osaka-u.ac.jp

Additional correspondence: Sacha Gnjatic, Ludwig Institute for Cancer Research, New York Branch, Memorial Sloan-Kettering Cancer Center, 1275 York Avenue, New York, NY 10065, USA.
e-mail: gnjatics@mskcc.org

Additional correspondence: Hiroshi Shiku, Departments of Cancer Vaccine and Immuno-Gene Therapy, Mie University Graduate School of Medicine, 2-174 Edobashi, Tsu, Mie 514-8507, Japan.
e-mail: shiku@clin.medic.mie-u.ac.jp

Received: 6/7/2012
Revised: 7/12/2012
Accepted: 28/1/2013
Accepted article online: 4/2/2013

frontiers in
IMMUNOLOGY

REVIEW ARTICLE
published: 11 July 2013
doi: 10.3389/fimmu.2013.00190

Natural and induced T regulatory cells in cancer

Dennis O. Adeegbe and Hiroyoshi Nishikawa*

Experimental Immunology, Immunology Frontier Research Center, Osaka University, Suita, Japan

Edited by:
Eyad Elkord, United Arab Emirates University, UAE, University of Salford and University of Manchester, UK

Reviewed by:
Axel Kallies, The Walter and Eliza Hall Institute of Medical Research, Australia
Yi-chi Kong, Wayne State University School of Medicine, USA
Nathan Karin, Technion – Israel Institute of Technology, Israel

***Correspondence:**
Hiroyoshi Nishikawa, Experimental Immunology, Immunology Frontier Research Center, Osaka University, 3-1 Yamadaoka, Suita, Osaka 565-0871, Japan
e-mail: nisihiro@ifrec.osaka-u.ac.jp

CD4+Foxp3+ T regulatory (Treg) cells control many facets of immune responses ranging from autoimmune diseases, to inflammatory conditions, and cancer in an attempt to maintain immune homeostasis. Natural Treg (nTreg) cells develop in the thymus and constitute a critical arm of active mechanisms of peripheral tolerance particularly to self antigens. A growing body of knowledge now supports the existence of induced Treg (iTreg) cells which may derive from a population of conventional CD4+ T cells. The fork-head transcription factor (Foxp3) typically is expressed by natural CD4+ Treg cells, and thus serves as a marker to definitively identify these cells. On the contrary, there is less consensus on what constitutes iTreg cells as their precise definition has been somewhat elusive. This is in part due to their distinct phenotypes which are shaped by exposure to certain inflammatory or "assault" signals stemming from the underlying immune disorder. The "policing" activity of Treg cells tends to be uni-directional in several pathological conditions. On one end of the spectrum, Treg cell suppressive activity is beneficial by curtailing T cell response against self-antigens and allergens thus preventing autoimmune diseases and allergies. On the other end however, their inhibitory roles in limiting immune response against pseudo-self antigens as in tumors often culminates into negative outcomes. In this review, we focus on this latter aspect of Treg cell immunobiology by highlighting the involvement of nTreg cells in various animal models and human tumors. We further discuss iTreg cells, relationship with their natural counterpart, and potential co-operation between the two in modulating immune response against tumors. Lastly, we discuss studies focusing on these cells as targets for improving anti-tumor immunity.

Keywords: Tregs, Foxp3, natural, induced, cancer, tumor, Interleukin-10, transforming growth factor β

INTRODUCTION

Early studies of T regulatory (Treg) cells, defined as a subset of CD4+ cells that co-express high levels of CD25, the high affinity IL-2 receptor α-chain, demonstrated unequivocally that these cells are crucial for maintenance of peripheral self tolerance as their elimination led to development of multiple organ-specific autoimmune diseases (1). Subsequent studies identified foxp3, a member of the fork-head/winged-helix family of transcriptional factor as uniquely expressed by Treg cells and allowed for more precise phenotypic identification of these cells as CD25 alone was insufficient due to its upregulation on activated T cells (1–3). Endowed with highly suppressive machinery, it is now well established that CD4+Foxp3+ Treg cells regulate a diverse array of immune responses ranging from autoimmune disease, allergies, and transplant rejection, to infections and cancers (4). While generally beneficial in the former conditions, the inhibitory activity of Treg cells often antagonizes protective immunity in the latter settings. Depending on the microenvironment in which they are found, and potential stimuli eliciting their recruitment or presence at such sites, CD4+Foxp3+ Treg cells are now broadly described as natural or adaptive (5, 6). Natural CD4+Foxp3+ Treg cells are the better understood of the two with the central dogma being that the adaptive or "induced" cells are generally derived from existing pool of naïve conventional CD4+ T cells. Regardless of their origin, they share one key feature: their ability to potently suppress effector T cells (5). Although expression of Foxp3 generally identifies natural, thymus-derived CD4+ Treg cells, adaptive Treg cells may or may not express this transcription factor (5, 7, 8).

Recent years have seen a surge in studies of cancer models and in humans highlighting the elevated levels of Treg cells in the tumor and/or in circulation (9, 10). This often correlates with poor anti-tumor effector response, hence compromised tumor immunity (11, 12). Whether the Foxp3+ cells widely described in many cancer settings are of natural or adaptive/induced type remains largely a bone of contention. This review focuses on the current knowledge about both subsets of Treg cells, their generation, phenotypic characteristics, and ill-defined roles as described in various tumor models and human cancers. Current therapeutic modalities geared toward Treg depletion and how they may impinge on recruited natural versus tumor-induced Treg (iTreg) cells are discussed.

INDUCED/ADAPTIVE TREGS, MORE THAN JUST Foxp3+ CELLS

Adaptive Tregs encompass a number of CD4+ cells with regulatory/suppressive capabilities (7, 8, 13). Although "iTregs" is commonly used interchangeably with "adaptive Tregs," the former is perhaps a better nomenclature for all extrathymically derived CD4+ Treg cells. In this context, iTreg cells range from Tr1 cells, which are induced by IL-10, and secrete both IL-10 and TGF-β (7), to TGF-β-producing Th3 cells (induced by oral antigen tolerizing